Feeding strategy as a key driver of the bioaccumulation of MeHg in megabenthos

David J. Amptmeijer¹, Andrea Padilla², Sofia Modesti², Corinna Schrum^{1, 2}, and Johannes Bieser¹

Correspondence: David J. Amptmeijer (davidamptmeijer@gmail.com)

Abstract. The bioaccumulation of methylmercury (MeHg) in the marine food chain poses a neurotoxic risk to human health, especially through the consumption of seafood. Although MeHg bioaccumulation at higher trophic levels is relatively well understood, MeHg bioaccumulation at the base of the food web remains underexplored. Given the neurotoxic effects of methylmercury on human health, it is essential to understand the drivers of bioaccumulation at every level of the food chain. In this study, we incorporate six megabenthos functional groups into the ECOSMO marine end-to-end ecosystem model, coupled to the MERCY marine Hg cycling model. We investigated how various feeding strategies influence the bioaccumulation of both inorganic Hg (iHg) and MeHg in marine ecosystems. We show that the feeding strategy significantly influences bioaccumulation and correlates stronger with iHg than the trophic level and that suspension feeders have elevated iHg levels while filter feeders have higher MeHg values. Additionally, we show that the bioaccumulation of both iHg and MeHg can be accurately modeled solely based on feeding strategies in low trophic-level megabenthos. However, when modeling higher trophic levels, incorporating the allometric scaling law dramatically improves the model performance. These results demonstrate the need for a holistic approach in which iHg, MeHg, and trophic levels of organisms are evaluated at both high and low trophic levels to identify what food web structures drive high MeHg concentrations in seafood.

1 Introduction

Mercury (Hg) is a naturally occurring element. In addition to its natural occurrence, it is also emitted through various anthropogenic activities, such as the burning of fossil fuels, small-scale artisanal gold mining, and the production of cement and ferrous metals (Pacyna et al., 2006). These anthropogenic emissions have significantly raised environmental Hg levels, with 78%, 85%, and 50% of atmospheric, upper ocean, and deep ocean Hg, respectively, originating from anthropogenic emissions (Geyman et al., 2025).

When elemental Hg (Hg⁰) is emitted, it can undergo long-range atmospheric transport. In this way, it can be transported on a global scale and deposited in the oceans, thus increasing Hg levels in the marine environment (Durnford et al., 2010). Marine Hg⁰ is volatile and can return to the atmosphere or be oxidized into dissolved Hg (Hg²⁺) (Sommar et al., 2020). This Hg²⁺ can be reduced back to volatile elemental Hg⁰, or it can be methylated to the dangerous neurotoxin methylmercury (MeHg), which occurs as monomethylmercury (MMHg⁺) or dimethylmercury (DMHg) (Jensen and Jernelov, 1969; Lin et al., 2021). In this

¹Matter Transport and Ecosystem Dynamics, Helmholtz-Zentrum Hereon, Geesthacht, Germany

²Universität Hamburg, Institute for Marine Sciences, Mittelweg 177, 20146 Hamburg, Germany

paper, we will look at the bioaccumulation of three groups of Hg; total Hg (tHg) refers to all Hg, methylmercury (MeHg) refers to both MMHg⁺ and DMHg, and inorganic Hg (iHg) refers to all Hg that is not MeHg.

There are two key processes involved in bioaccumulation: bioconcentration and biomagnification. When animals absorb Hg directly from their environment, this is called bioconcentration. Both iHg and MeHg bioconcentrate. Since iHg is generally present in higher concentrations than MeHg, and its bioconcentration rate is higher, iHg is usually bioconcentrated faster than MeHg (Mason et al., 1996). The bioconcentration process can result in high concentrations in aquatic organisms. This process is commonly quantified using the Volume Concentration Factor (VCF), a unitless ratio between the Hg concentration in phytoplankton and that in the surrounding water:

$$VCF = \frac{C_{\text{phytoplankton}}}{C_{\text{water}}} \tag{1}$$

where both $C_{\text{phytoplankton}}$ and C_{water} have the same units, for example, ng Hg μ m⁻³, and the VCF is unitless. For MeHg, very high volume concentration factors of up to 6.4×10^6 have been reported in the literature (Lee and Fisher, 2016; Schartup et al., 2018).

MeHg concentrations that are elevated due to bioconcentration can be further increased by biomagnification along the aquatic food web. Biomagnification refers to the increase in Hg with each successive trophic level in the food chain. The trophic transfer efficiency of MeHg (66-80%) is higher than that of iHg (7-46%), where MeHg accumulates at much higher levels in the food chain (Metian et al., 2020; Wang and Wong, 2003; Dutton and Fisher, 2012). MeHg is a neurotoxin whose overconsumption can decrease IQ points and raise the risk of heart attacks, and consumption of MeHg-contaminated seafood is the primary pathway of Hg exposure in humans, with elevated risk among coastal and seafood-reliant populations (Sheehan et al., 2014; Zhang et al., 2021; Genchi et al., 2017; Trasande et al., 2006).

The risk associated with consuming seafood contaminated with MeHg gained significant attention after over 1000 fatalities occurred in Japan in 1956 due to the consumption of contaminated seafood from Minamata Bay (Harada, 1995). Although this MeHg outbreak was a unique event linked to industrial waste disposal containing Hg, it highlighted the dangers of MeHg exposure. In order to reduce the risk of further outbreaks of MeHg intoxications, the Minamata Convention on Mercury was founded. A total of 151 countries have pledged to reduce their Hg emissions in support of the Minamata Convention and 128 countries have signed and ratified the convention (UNEP, 2013). The global state of Hg as a pollutant and the effect of the Minamata Convention is periodically reviewed in the Minamata Convention Effectiveness Evaluation (Outridge et al., 2018).

While there is considerable understanding of MeHg bioaccumulation in high trophic levels, less is known about the bioaccumulation drivers at the base of the food web where Hg concentrations tend to be lower, resulting in reduced risk to humans. As such, these organisms are not prioritized in the current monitoring strategies under the ongoing effectiveness evaluation of the Minamata Convention, which focuses primarily on fish, humans, and predatory wildlife (Evers et al., 2016). Additionally, the evaluation to date has shown that Hg and MeHg concentrations in water and sediment do not correlate well with levels in biota, leading to greater emphasis on biological monitoring over abiotic compartments.

Once Hg is bioconcentrated in primary producers, a strong link appears between the trophic level and Hg bioaccumulation (Madgett et al., 2021). This indicates that our understanding of Hg bioaccumulation in high trophic levels is greatly limited by our understanding of Hg bioaccumulation at the base of the food web.

60

80

The benthic food web is highly complex, making it challenging to improve our understanding of bioaccumulation within it (Silberberger et al., 2018). There are several distinct groups of megabenthos with different feeding strategies, such as bivalves that filter feed, lugworms that feed on sediment carbon particles, active hunters and scavengers such as shrimps and crabs, and sponges that feed on suspended dissolved material. These different feeding strategies allow them to exploit a variety of food sources, but different food sources can have different Hg concentrations, and Hg originating from different food sources can have different assimilation efficiencies. In this study, we hypothesize that the low-trophic-level biota feeding strategy has a significant impact on their Hg content.

We focus this study on the benthic food web. Although primary production in the North Sea can be highly variable due to factors such as wind (Daewel and Schrum, 2017), tidal mixing (Zhao et al., 2019) and nutrient availability (Richardson et al., 1998), primary production in coastal areas is generally dominated by pelagic phytoplankton, with the exception of extremely shallow areas that are dominated by benthic macroalgae (Krause-Jensen et al., 2012; Cibic et al., 2022). In well-mixed areas where pelagic phytoplankton dominate primary production, they can be consumed by megabenthos and there is a strong coupling between the benthic and the pelagic, called the bentho-pelagic coupling. In these well-mixed areas, megabenthos can reach high biomass since food is abundant in several ways, resulting in megabenthos with different feeding strategies in the same ecosystem (Ghodrati Shojaei et al., 2016).

We hypothesize that the different feeding strategies of low-trophic-level megabenthos play an important role in creating the disconnect between Hg concentrations in the water and sediment and the concentrations at the base of the food web. We investigated whether the feeding strategy impacts bioaccumulation and hypothesized that feeding strategies influence the bioaccumulation of iHg and MeHg differently, contributing to the high variation in Hg levels at the base of the benthic food web.

To test our hypotheses, we employed three approaches. First, we conducted a literature review in which we collected field observations of tHg, MeHg, and iHg concentrations, together with trophic level and megabenthos feeding strategy. We then performed statistical analyses on these data to examine if we could find a relationship between feeding strategy and trophic level. Second, we carried out a modeling experiment in which megabenthos with different feeding strategies competed under physical drivers in idealized scenarios representative of megabenthos-rich coastal oceans. The megabenthos groups were designed to differ only in their feeding strategies, allowing us to isolate this effect. This experiment was used to test whether the observed effects from our literature review could be reproduced in a fully coupled model.

Finally, we analyzed data from a single study to evaluate whether the same dynamics observed in the model and the global dataset were also present in a single geographical location. While none of these individual tests is conclusive on its own, consistent evidence across all three approaches would support the conclusion that feeding strategy is an important driver of Hg bioaccumulation and would warrant further empirical studies to investigate this role in more detail.

2 Materials and methods

2.1 The models

To assess the importance of the feeding strategy, we modeled bioaccumulation in megabenthos, with the feeding strategy being the only distinction between different groups of megabenthos. Then we compared our model to observations to evaluate whether this approach allows us to accurately model bioaccumulation or if additional drivers should be taken into account. We used a fully coupled 1D water column model that is run in 2 setups that resemble typical hydrological regimes found in coastal oceans. We coupled the Generalized Ocean Turbulence Model (GOTM) (Burchard et al., 1999) with the ECOSMO E2E ecosystem model (Daewel et al., 2019) and the MERCY v2.0 Hg speciation and bioaccumulation model (Bieser et al., 2023).

2.1.1 The hydrodynamical model

The hydrodynamics of the model are estimated using the GOTM, which is a 1D hydrodynamic model (Bolding et al., 2021). GOTM calculates the turbulence of a vertical 1D water column set-up by computing the solutions to the one-dimensional version of the transport equation of momentum, salinity, and temperature. The model is nudged to observational data sets for temperature and salinity. The setups are based on gridded bathymetry data for water depth with 1/240° resolution (GEBCO Bathymetric Compilation Group, 2020), ECMWF ERA5 dataset for meteorological data (Wouters et al., 2021), Ocean Atlas for salinity and temperature profiles (Garcia H.E. et al., 2019), and the TPOX-9 atlas for tides (Egbert and Erofeeva, 2002), which is combined using the iGOTM tool (https://igotm.bolding-bruggeman.com). The GOTM model is coupled using the Framework for Aquatic Biogeochemical Modeling (FABM) (Bruggeman and Bolding, 2014). The biogeochemical models are encoded in FABM. The FABM interfaces communicate the state variables between the GOTM model and the biogeochemical models.

110 2.1.2 The physical setups

120

The model runs in 2 setups, the first is a 41.5 m deep permanently mixed Southern North Sea set of 41.5 m deep and the second is a seasonally mixed 110 m Northern North Sea setup. These setups are described in more detail in Amptmeijer et al. (2025). The Southern North Sea setup is located at $(54^{\circ}15'00.0"N\ 3^{\circ}34'12.0"E)$. It is a shallow station that is permanently mixed, meaning that megabenthos can feed directly from the phytoplankton and zooplankton bloom. The setup is chosen because it resembles perfect growth conditions for megabenthos, and most megabenthos in the observations are sampled from similar circumstances. Because of this, most samples are from shallow well-mixed coastal areas, and we used this setup to evaluate the performance of the models.

The Northern North Sea setup is located at $(57^{\circ}42'00.0"N\ 2^{\circ}42'00.0"E)$ and is only mixed in winter. This means that megabenthos cannot feed directly from the bloom, but are rather dependent on the sinking of detritus particles. In nature, these deeper areas typically have lower overall biomass. This setup is used to evaluate whether the models predict a difference in the bioaccumulation of iHg and MeHg under a different hydrodynamic regime.

2.1.3 The MERCY v2.0 model

Hg cycling and speciation is modeled using the MERCY v2.0 model (Bieser et al., 2023). The MERCY v2.0 model is a comprehensive Hg cycling model that includes speciation between 7 forms of Hg and partitioning to both dissolved organic matter (DOM) and detritus. It was originally developed as a 3D Hg cycling model of the North and Baltic Seas. However, in this study, we use the 1D version of this model, which is driven using the GOTM model. This configuration is used, described, and evaluated in more detail in (Amptmeijer et al., 2025).

2.1.4 ECOSMO E2E

125

130

135

145

150

The ecosystem model is based on the ECOSMO E2E (ECOSystem Model End-to-End) ecosystem model (Daewel et al., 2019). This model extends the ECOSMO II model to have higher trophic levels while preserving consistency at lower trophic levels (Daewel et al., 2019). The version used in this study is the same as the version used and evaluated in (Amptmeijer et al., 2025). In this version, small modifications have been made, such as lowering the mortality rate of zooplankton and decreasing the efficiency of carbon uptake to make the model more suitable for bioaccumulation compared to the version published by (Daewel et al., 2019). Bioaccumulation is implemented to account for bioconcentration in all trophic levels and biomagnification in all consumers. Phytoplankton have a size-dependent uptake and release rate for the uptake and release of iHg. Based on observations by Pickhardt et al. (2006) that found higher MeHg in smaller phytoplankton but consistent iHg levels, phytoplankton have a size-dependent uptake rate and constant release rates. This means that diatoms and flagellates bioaccumulate similar amounts of iHg, while the smaller flagellates accumulate more MeHg. The uptake and release rates of iHg and MeHg in zooplankton are based on Tsui and Wang (2004) and on Wang and Wong (2003) for fish. An essential component of the ecosystem that interacts with bioaccumulation in megabenthos that was not overhauled for this study is the interactions between detritus and DOM and iHg and MeHg. The only Hg species assumed to partition to DOM an detritus are Hg²⁺ and MMHg⁺, and this partitioning is assumed to be an equilibrium that is instantaneous and is reestimated on every time step. The equilibrium is based on the K_{dw} values which are based on Allison et al. (2005) and Tesán Onrubia et al. (2020). This value is $\log_{10}(6.4)$ and $\log_{10}(6.6)$ for the partitioning of Hg²⁺ and $\log_{10}(5.9)$ and $\log_{10}(6.0)$ for the binding of MMHg⁺ to detritus and DOM respectively. This is the same approach that is used and evaluated in Bieser et al. (2023).

2.2 Model development

To use the model to study bioaccumulation in megabenthos, the higher trophic level of the ECOSMO E2E model is altered. We exchanged the functional group macrobenthos, fish 1, and fish 2 with 6 megabenthos functional groups, as shown in Fig. 1. The megabenthos groups are separated by their feeding strategy: filter feeder, deposit feeder, generalist feeder, suspension feeder, predator, and top predator.

Filter feeders filter suspended particles from the water column. In our model, they can eat phytoplankton, zooplankton, and detritus. Examples of filter feeders are mussels, tubeworms, and barnacles. The second group is **deposit feeders**. These animals consume organic carbon from the sediment; in our model, they exclusively feed on organic carbon deposited in the sediment.

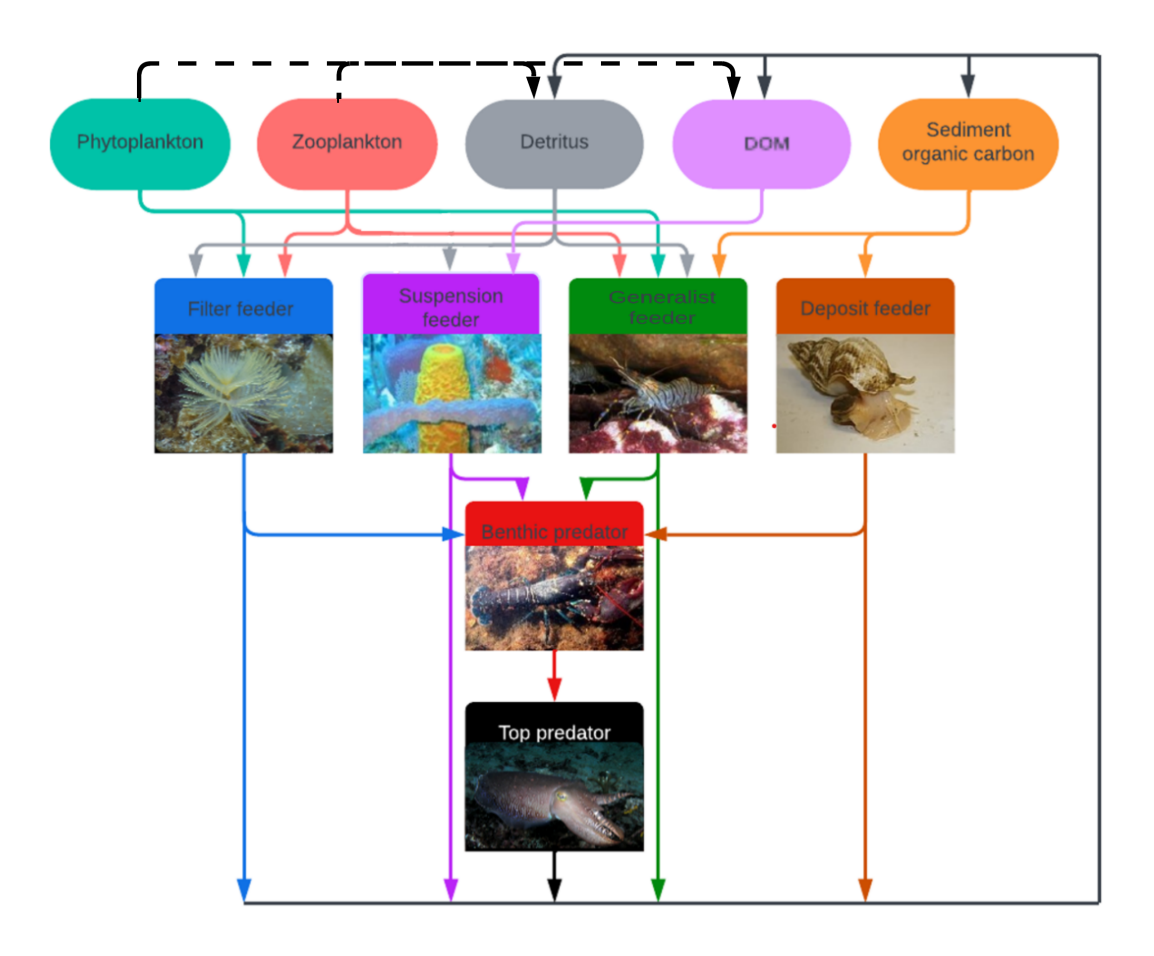


Figure 1. The overview of the modeled megabenthos functional groups and how they interact with each other and functional groups in the ECOSMO E2E model. There are 5 megabenthic functional groups. The filter feeder feeds on pelagic detritus, zooplankton, and phytoplankton. The suspension feeders feed on pelagic detritus, phytoplankton, zooplankton, and DOM. The generalist feeds on phytoplankton, zooplankton, pelagic detritus, and sediment organic carbon. The deposit feeder feeds on sediment organic carbon. The benthic predator feeds on the other 4 megabenthos functional groups and the top predator solely feeds on the benthic predator. The arrows indicate trophic interactions where the arrow goes from the prey to the predator and the arrows have the same colour as the prey. The black lines represent loss of organic material due to mortality. When megabenthos die, their organic carbon is transferred to pelagic DOM and detritus, as well as the sediment, shown by the solid black arrow. In contrast, when pelagic organisms die, their organic carbon is transferred to DOM and detritus, indicated by the dotted black arrow. Several sub-images have been used in this image. Sources of the images: Filter feeder: *Sabella spallanzanii* (photo by Diego Delso, CC BY-SA 4.0, via Wikipedia), Suspension feeder: *Aplysina fistularis* (photo by Twilight Zone Expedition Team 2007, NOAA-OE, CC BY 2.0, via Flickr), Generalist feeder: *Crangon crangon* (photo by Etrusko25, Public Domain, via Wikipedia), Deposit feeder: *Buccinum undatum* (photo by Oscar Bos / Ecomare, CC BY 4.0, via Wikipedia), Benthic predator: *Hommarus gammarus* (photo by Bart Braun, Public Domain, via Wikipedia), Top predator: *Sepia officinalis* (photo by Nick Hobgood, CC BY-SA 3.0, via Wikipedia).

This group would include gastropods and polychaete worms, such as the lugworm (*Arenicula marina*). The **generalist feeder** resembles animals such as brown shrimp (*Crangon crangon*), which can utilize various feeding strategies. In our model, this group feeds on phytoplankton, zooplankton, detritus, and deposited material. We also include a **suspension feeder**. Suspension feeders, such as sponges, can consume detritus and DOM. The consumption of DOM, which is too small to be consumed by filter feeders, differentiates suspension and filter feeders. A common strategy to consume DOM as a food source is the utilization of symbiotic bacteria such as chemosymbiotic bivalves from the families Lucinidae, Solemyidae, and Thyasiridae, and microbial biomes of high microbial assemblage sponges (Dufour, 2018; Olinger et al., 2021). Finally, we included 2 predators. The first predator is referred to as **the predator**, it feeds on the 4 benthic groups mentioned above, and it has an equal preference and grazing rate in all groups, but it will prioritize abundant groups. This preference is caused by making the food available for predation by the predators not linearly related to the abundance of the prey, but calculated as:

$$b_{\text{available}} = \begin{cases} b_{\text{biomass}}, & \text{if } b_{\text{biomass}} \ge b_{\text{protected}}, \\ b_{\text{biomass}} \frac{b_{\text{biomass}}}{b_{\text{protected}}}, & \text{if } b_{\text{biomass}} < b_{\text{protected}}. \end{cases}$$

165 in which,

180

- $b_{\text{available}}$: Portion of prey biomass in g C m⁻² accessible to predators.
- $b_{\text{protected}}$: Level of prey biomass in g C m⁻² below which hunting becomes less optimal or energetically inefficient.
- b_{biomass} : Total prey biomass in g C m⁻² in the environment.

The megabenthos in the North Sea are estimated to have between 1.1 and 35.5 gC m⁻² (Heip et al., 1992; Daan and Mulder, 2001). The value for B_{Protected} is chosen as 1 gC m⁻² for all megabenthos except for the benthic predator where B_{Protected} is 0.5 gC m⁻². These values are chosen to protect megabenthos functional groups from extinction due to predation when their values are below the expected range. This relationship models 2 real-world interactions. First, when the concentration of prey is low, the small number of individuals can more likely survive under ideal circumstances and, therefore, may be less exposed to predation (Campanella Id et al., 2019). Secondly, several predators, such as the shore crab, adapt their behaviors to the density of the prey and learn to be more efficient in the hunting of more common prey (Chakravarti and Cotton, 2014). Our model is resolved in carbon content, while measurements are often in dry weight. The carbon fraction of dry weight generally ranges from 0.4 to 0.6, but can vary between different taxa (Gorokhova and Hansson, 2000; Jurkiewicz-Karnkowska, 2005). To ensure consistency across different functional groups with diverse feeding strategies, we maintain a 1:2 conversion ratio for carbon to dry weight for all megabenthos functional groups.

2.2.1 Assimilation efficiency of iHg and MeHg

The assimilation efficiency (AE) of iHg and MeHg is a key parameter in correct biomagnification modeling. AE is based on laboratory experiments that analyze AE in phytoplankton (Metian et al., 2020; Wang and Wong, 2003). An assimilation efficiency of 0.95 for MeHg and 0.31 for iHg is chosen for everything except deposit feeding, which has a lower feeding efficiency of 0.07 for iHg and 0.43 for MeHg according to Dutton and Fisher (2012).

2.2.2 Semi-labile DOM

185

200

205

In the ECOSMO E2E model, only labile-DOM is resolved. This means that there is very little DOM. In our model, we want to incorporate a suspension feeder that would utilize DOM as a food source. Because of this, we added a DOM component referred to as semi-labile DOM. This semi-labile DOM has the same bacterial degradation rate as that of the detritus, and it has the same Hg partitioning behavior as labile DOM. When organic carbon (detritus+labile-DOM+semi-labile-DOM) is formed, 5% is formed as semi-labile DOM, and there is a breakdown of the detritus into semi-labile DOM of 0.001 d⁻¹ (per day). Since the categorization of DOM is very complex, these rates are estimated to create a low maximum of 50 mg C m⁻³. This is lower than the DOM concentrations typically found in the North Sea, but because it is unclear which fraction of DOM can be consumed by suspension feeders, this amount provides suspension feeders a unique food source that they can utilize while not outcompeting other megabenthos (Lønborg et al., 2024).

195 2.2.3 Allometric scaling model

Finally, we run the model while taking into account other drivers of MeHg bioaccumulation to see whether it improves the model. There are three interactions that we take into account for this second model. First, the allometric scaling law, which states that larger animals have a lower base metabolic rate when normalized to body weight (da Silva et al., 2006). Secondly, we account for the observations that MeHg bioaccumulation in fish increases as the water temperature increases, indicating that increased activity does not increase MeHg excretion while it increases MeHg uptake due to a higher grazing rate (Dijkstra et al., 2013). Finally, we assume that predators need to spend more energy on active metabolism to hunt their prey. Because of this, we assumed that the total relative respiration rate of predators and top predators is not altered, so both models have the same carbon cycle. However, MeHg is excreted at a lower rate of 0.002 d⁻¹, rather than their respiration rate, which is the same base metabolic rate as the fish in the ECOSMO E2E model. This leads to a higher bioaccumulation of MeHg at higher trophic levels. The bioaccumulation of iHg is not altered between the two models. In the evaluation, the second model is referred to as the allometric scaling (AS) model.

2.3 Literature research and statistics

2.3.1 Literature research

To compare the findings with the literature, we collected field studies measuring Hg in megabenthos. The studies we used are shown in Table S1. We categorized the megabenthos into the same feeding categories, "deposit feeder", "filter feeder", "suspension feeder", "grazer", and "predator". To better assess the effect of the trophic level, we also added "primary producers" as the base of the food web, and "seabird" and "benthic fish" as top predators. We analyzed whether trophic level and feeding strategy influence megabenthos iHg, MeHg, and/or tHg content. The total and partial R² of the linear regression of the trophic level and the feeding strategy were compared to analyze the effect of both drivers on bioaccumulated iHg, MeHg, and tHg.

We compared our model to observations in two ways. First, we compared it to all the data available in our global dataset. We acknowledge the limitation of this approach, as different geographical regions may have different Hg baselines, but it can provide insight into whether certain feeding strategies are consistently higher or lower in iHg, MeHg, or tHg. The most comprehensive dataset of MeHg bioaccumulation that we could find was published by McClelland et al. (2024), we used this single dataset to verify if patterns observed in the model and the global dataset are also present in a single dataset. If certain patterns are present in our model, in globally aggregated data, and in a single large dataset, it becomes a compelling argument to form a hypothesis for further targeted empirical studies.

2.3.2 Model evaluation using a global dataset

225

230

235

245

The goal of the model is to evaluate how well we can represent the bioaccumulation of iHg and MeHg while only taking into account the feeding strategy and trophic interactions. To this extent, the model's result is its performance. If the model performs well, we can conclude that only accounting for feeding strategies and trophic interactions explains a large amount of the variability in Hg bioaccumulation. Initially, we performed this comparison between observations and the modeled Southern North Sea setup. This was done because most samples are collected from shallow areas with high megabenthic biomass, which the well-mixed Southern North Sea setup better resembles. Afterwards, the models were compared to the Northern North Sea models and the AS model to evaluate the effect of hydrodynamics and increased bioaccumulation in higher trophic level animals on our conclusions. The grazer feeding strategy was omitted, as the ECOSMO E2E model does not include benthic algae to graze on. The modeled generalist was compared to the sum of the deposit and filter feeders from the observations, and the modeled top predator to the benthic fish and seabird feeding strategies.

Model performance was evaluated using normalized bias, RMSE, NRMSE, and the R^2 (Pearson and residual) (see Table S2 for details). Normalized bias and NRMSE values below 0.5 indicate low bias and a good fit. $R^2_{\rm Pearson}$ quantifies how well differences between feeding strategies are captured, while $R^2_{\rm Residual}$ reflects agreement with absolute observed values.

2.3.3 Evaluation of the model using a single dataset

We used MeHg bioaccumulation and trophic level data from 476 individuals across 53 taxa of benthic invertebrates as published by McClelland et al. (2024) to verify if the interactions that occur in both our model and the global dataset are consistent when data from 1 geographical location is studied. These data were selected as they are the largest study we could find with both trophic level and MeHg concentrations. When several animals of the same group were sampled, the dataset presents mean values per group per location, which we use as one datapoint in our analyses. Although feeding strategies in the dataset were broadly aligned with our classifications, we reassigned them to match the functional groups in our model. For example, shrimps were categorized as generalist feeders, which group is not present in McClelland et al. (2024), and isopods, which can be small benthic predators, were labeled as deposit feeders because their prey type is not represented in our model.

The data is sampled from two locations in the Canadian Arctic, Cape Bathurst (CB), which has a depth of 22 m and is located at 70°41′42.79″ N, 128°50′21.34″ W, and the eastern coast of Herschel Island in the Mackenzie Trough (MT), which has a depth of 116 m and is located at 69°36′44.96″ N, 138°33′45.25″ W. It must be noted this dataset is selected as it is extensive,

but the region does have notable differences to the North Sea, where our model is run. It has extensive ice cover in winter, it is colder, and is geographically distant from the model location. It does, however, provide us with an opportunity to test if our model conclusions can be verified using field observations from a single study.

To isolate the effect of the feeding strategy on MeHg bioaccumulation, we first transformed MeHg concentrations to their natural logarithm and fit a linear model with trophic level as predictor using the base R lm() function. The significance of the deviation from the predicted MeHg concentration at the trophic level was assessed using a one-sample t test. To improve interpretability, we calculated the percentage differences using Percentage difference = $100 \times \left(\frac{MeHg_{obs}}{MeHg_{pred}} - 1\right)$ based on the residuals of the linear fit. This is visualized on a bar graph showing the percentage difference in MeHg concentration caused by the feeding strategy. The error bars represent the 1 Standard Error (SE). The same analysis was then performed to estimate differences in MeHg bioaccumulation related to phylum.

As a final test, linear models were fitted on the natural logarithm of bioaccumulated MeHg concentrations using trophic level, phylum, and feeding strategy as predictor variables (using the lm() function in R). Estimated marginal means (EMM) for each feeding strategy were calculated with the emmeans () function of the emmeans package and compared against the overall mean to assess deviations. This analysis was also performed separately for the MT and CB locations to verify the consistency of the effects of the feeding strategy. The EMMs were transformed to a percentage difference with the earlier used equation and the estimated percentage difference due to feeding strategy and its significance is shown.

3 Results

250

255

260

265

3.1 Model evaluation

3.1.1 Evaluation of the Hg cycling and pelagic bioaccumulation

The marine cycling and speciation of Hg, in addition to the bioaccumulation in phytoplankton and zooplankton, is an essential driver of the bioaccumulation of iHg and MeHg in the benthic food web. Observed and modelled dissolved tHg concentration, the percentage of tHg that is MeHg, and the Hg content of phytoplankton and zooplankton is shown in Table 1. The concentration of dissolved tHg and the percentage of MeHg of dissolved tHg are compared to observations by Coquery and Cossa (1995), while the bioaccumulation of tHg in phytoplankton and zooplankton is compared to observations by Nfon et al. (2009). It must be noted that the observations by Nfon et al. (2009) are not from the North Sea itself, but from the better-studied nearby Baltic Sea. The average dissolved tHg concentration is 1.7 and 2.1, pM in the Northern and Southern North Sea, respectively. This is well within 1 standard deviation of the 1.7 ± 0.7 pM observed by Coquery and Cossa (1995). The MeHg concentration was observed to be between 0.5 and 4.3% of tHg, with an average of 3% in the North Sea. The percentage MeHg in our model is 2.3% and 2.0% on average, which falls well within that range.

For bioaccumulation, we could not find separate reliable measurements of MeHg and iHg in phytoplankton and zooplankton in the North Sea, and we therefore evaluated the tHg content. This was measured in diatoms to be 10 ± 5 ng Hg mg⁻¹. This means that the mean bioaccumulation in our model in diatoms is lower, with 5.8 ng Hg mg⁻¹ and 9.0 ng Hg mg⁻¹ in the

Northern and Southern North Sea, respectively, but still within 1 standard deviation of the measurements. Observations labeled as zooplankton and mysis were compared to our modeled microzooplankton and mesozooplankton, respectively. All modeled values fall within 1 standard deviation of the observed tHg concentration, with one exception: mesozooplankton in the Northern North Sea, which is 13.5% more than 1 standard deviation above the observations. This is mostly driven by a high iHg content, as the MeHg content is similar in microzooplankton and mesozooplankton.

This similarity in the MeHg content of microzooplankton and mesozooplankton in our model is caused because, even though mesozooplankton have a higher trophic level, they prefer to feed on larger diatoms which have a lower MeHg bioconcentration rate than smaller flagellates, which are preferred by microzooplankton. The high iHg content, especially in the Northern North Sea, is caused by the consumption of detritus by zooplankton in the model. While there is a shortage of data on bioaccumulation at the base of the food web, especially in the North Sea, which complicates model evaluation, the dissolved tHg concentration, the percentage of MeHg, and the tHg content of phytoplankton and zooplankton agree well with observations. With the exception of the 13.5% elevated tHg content in Northern North Sea mesozooplankton, all modeled values fall within 1 standard deviation of the observations. Because of this, we conclude that the model replicates marine Hg cycling and bioaccumulation at the base of the food web in line with observations, with the caveat that we do not have measurements of zooplankton in the Northern North Sea to verify or reject the elevated levels in that setup.

Table 1. Dissolved tHg (pM), MeHg (% of tHg), and tHg concentrations in biota (ng Hg mg⁻¹ d.w.) across North Sea regions.

	Observed	NNS	SNS
tHg _{dissolved} (pM)	1.7 ± 0.7	1.7 ± 0.26	2.0 ± 0.28
MeHg (% of tHg)	3 (0.5–4.3)	2.3 ± 0.23	2.0 ± 0.31
Diatoms tHg (ng Hg mg ⁻¹)	10 ± 5	7.0 ± 1.1	8.3 ± 1.6
Flagellates tHg (ng Hg mg ⁻¹)		13.9 ± 3.0	14.3 ± 3.0
Microzooplankton tHg (ng Hg mg ⁻¹)	37.5 ± 31.3	67.4 ± 29.3	40.3 ± 11.4
Microzooplankton MeHg (ng Hg mg ⁻¹)		7.1 ± 2.1	10.5 ± 2.7
Mesozooplankton tHg (ng Hg mg ⁻¹)	62.5 ± 12.5	86.7 ± 15.1	72.3 ± 19.6
Mesozooplankton MeHg (ng Hg mg ⁻¹)		6.9 ± 2.6	10.5 ± 1.7

3.1.2 Megabenthic biomass

285

290

295

While our megabenthos groups only vary in their feeding strategies and lack a direct real-world counterpart, it is important to ensure that all functional groups have consistent biomass in the model and thus the results originate from the modeled interactions, and are not altered due to unrealistically high or low modeled biomass. The yearly progression of the megabenthos biomass is shown in Fig. 2. Filter feeders have the highest biomass, which is up to 10 g C m⁻² followed by deposit feeders with up to 5 g C m⁻², generalist feeders with up to 3 g C m⁻², and suspension feeders with up to 1 g C m⁻². Higher trophic levels have

lower biomass, with up to 0.2 g C m⁻² for the predator and 0.5 g C m⁻² for the top predator. This shows that after a simulation period of 20 years, all megabenthos have a stable population, while biomass is highest at the base of the food web.

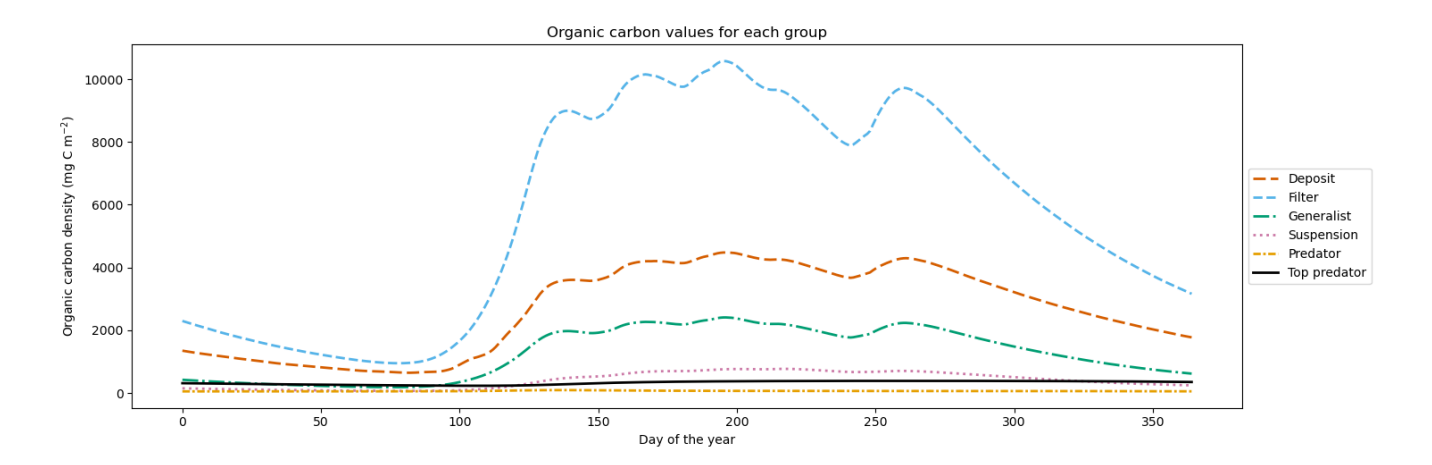


Figure 2. Megabenthos biomass in the modeled Southern North Sea, dominated by filter feeders, followed by deposit feeders, generalist feeders, suspension feeders, predators, and top predators. Biomass fluctuates between 10 and 15 gC m⁻² and all functional groups have stable populations

3.2 Bioaccumulation in the model

The modeled bioaccumulation in the AS model in the Southern North Sea is shown in Fig. 3, note that the values are expressed in ng Hg mg C^{-1} , as this is the best proxy in our model to show the dietary uptake of Hg per energy and nutrients consumed. There is a very high concentration of iHg in the sediment, detritus, and DOM. These values are 0.60, 1.1, and 2.6 ng Hg mg C^{-1} for iHg and 0.089, 0.0067, and 0.012 ng Hg mg C^{-1} for MeHg. The high amount of iHg in organic carbon is in line with observations that found values of up to 0.114-1.192 ng Hg mg d.w. in sediment in the Scheldt estuary and that DOM strongly binds up to 1.0 ng Hg mg⁻¹ (Zaferani and Biester, 2021; Haitzer et al., 2002; Muhaya et al., 1997), which would approximate our modeled 2.6 ng Hg mg C^{-1} if we assume a carbon to weight ratio of 1:2. These high iHg values in DOM lead to high values in suspension feeders in both setups. The bioaccumulation of MeHg is very different from that of iHg and has the highest bioaccumulation in the top predators and predators, followed by deposit feeders and suspension feeders. In Fig. 4a, c, and e the relationship between the trophic level and the bioaccumulation of iHg, MeHg, and tHg in megabenthos in the model is shown. There is an increase in the MeHg content with trophic levels that are not present for iHg. For iHg, there is weak anti-correlation ($R^2 = 0.20$), which is mainly caused by the extremely high iHg content of the low-trophic-level suspension feeders. There is no positive relationship between the bioaccumulation of tHg and the trophic level ($R^2 = 0.02$), while this is present in the AS model ($R^2 = 0.50$); this indicates that our base model underestimates the bioaccumulation at higher trophic levels.

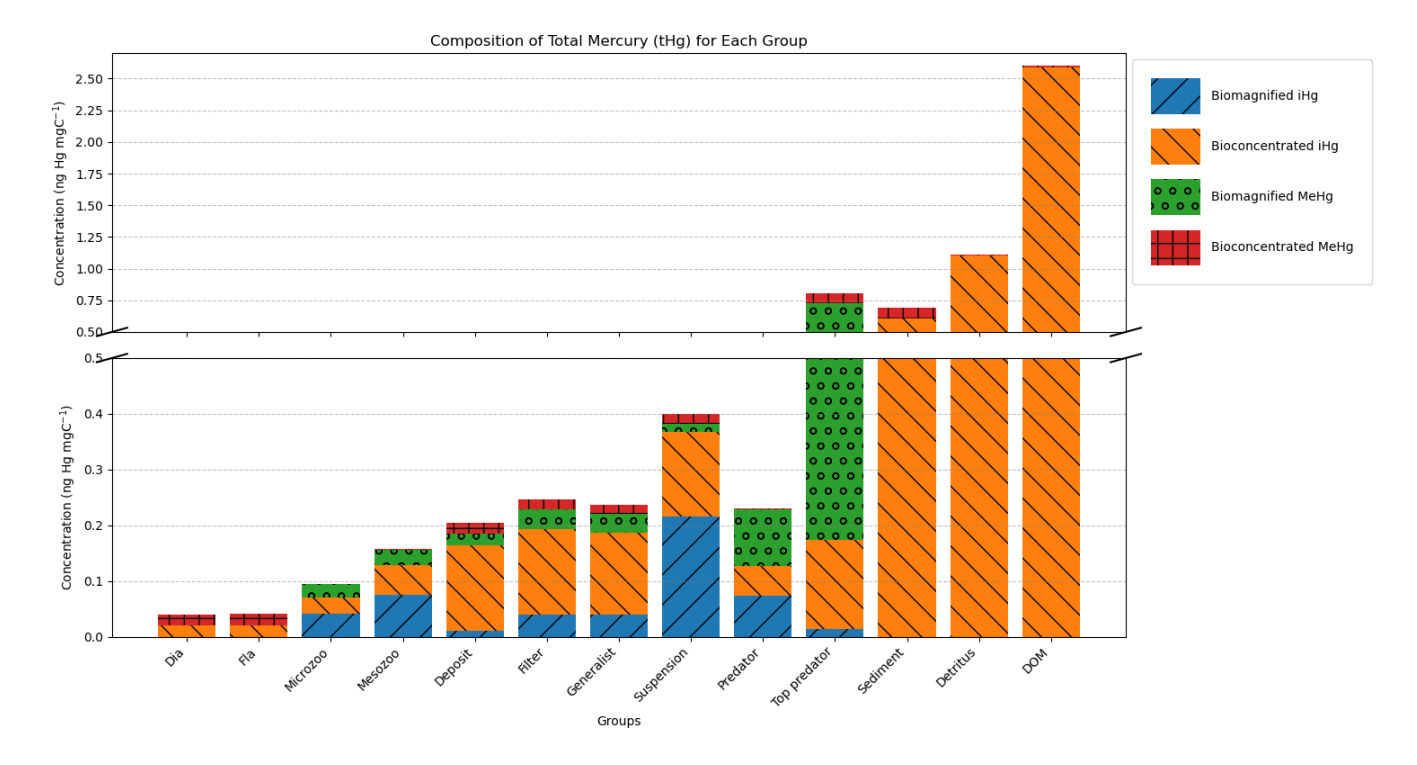


Figure 3. Modeled bioconcentration and biomagnification of iHg and MeHg. Partitioning to detritus and DOM is colored as bioconcentration. The y-axis is cut to show the high and low values. Notably is the high iHg to mgC ratio of detritus and DOM, leading to elevated iHg in suspension feeders. Additionally, higher trophic level animals have higher biomagnified MeHg

3.3 Bioaccumulation in the gobal dataset

320

325

In Table 2 we show the results of a linear regression using the global dataset taking into account both the trophic level and the feeding strategy; the relative fit of each model explains Hg bioaccumulation based on both factors. The trophic level and feeding strategy are adapted to the natural logarithms of iHg, tHg, and MeHg. This shows that we can explain the bioaccumulation of ln(MeHg) very well (R^2 =0.72) with a linear model that takes both drivers into account, while the bioaccumulation of iHg is poorly explained (R^2 =0.11) and the bioaccumulation of tHg has an average fit (R^2 =0.46). Furthermore, we show the unique contributions of the fit of each driver, the partial R^2 . Note that feeding strategy and trophic level can sometimes co-correlate, especially in the case of high MeHg bioaccumulation in predators, benthic fish, and seabirds, as predators are naturally higher in trophic level than the prey they consume. The feeding strategy has an explanatory power larger than that of the trophic level for tHg and iHg, while it is similar for MeHg. Despite the limitations mentioned above, this still shows that the partial R^2 for the feeding strategy is double that of the trophic level, demonstrating the importance of the feeding strategy for the bioaccumulation of tHg at the base of the food web.

Table 2. R-squared and Partial R-squared Results for ln(THg), ln(iHg), and ln(MeHg)

Model	ln(tHg)	ln(iHg)	ln(MeHg)
Full Model R-squared	0.46	0.11	0.72
Partial R-squared (Feeding Strategy)	0.22	0.089	0.32
Partial R-squared (Trophic Level)	0.10	0.012	0.31

330 3.4 The allometric scaling law in high trophic level animals

In Table 3 we show the model performacne against the global dataset of the base and the AS model. This shows that if we take the allometric scaling law into account, the model results for high-trophic level animals increase considerably. In Fig. 4b, d, and e we show the relation between the natural logarithm of bioaccumulation and the trophic level of the AS model in the Southern North Sea setup. The normalized bias in the predator and top predators decreased from -0.37 and -0.82 to -0.26 and -0.24, respectively. Our base model does agree well with both observed iHg (R^2 =0.84) and MeHg (R^2 =0.86) in the Southern North Sea setup, but this is mostly driven by accurate predictions in the lower trophic levels while there is a normalized bias of -0.84 in the Top Predators. This is improved dramatically in the AS model with the reduction of the normalized bias of top predators to -0.32 which improves the overall R^2 of the model to >0.99.

3.5 Comparing model and observations

335

345

350

340 3.5.1 The effect of feeding strategy on bioaccumulation

The mean annual average and range of the bioaccumulation of iHg and MeHg in our model and the range and mean of measured iHg and MeHg are shown in Table 4. We additionally visualised in Fig. 5 the modeled values of the AS model in the Southern North Sea compared to the observations. In Fig. 5a the bioaccumulation of MeHg and in Fig. 5b the bioaccumulation of iHg is visualised. All values fall within the range of observations, except for the modeled top predator in the base model. In the AS model, the top predator has values for both iHg and MeHg in both the Southern North Sea and the Northern North Sea that are within the range of observations. The most notable observation for iHg bioaccumulation is that, although the variation in measured iHg is considerable, suspension feeders consistently have high iHg values. In both the Southern North Sea setup and the observation the mean MeHg is lowest in suspension feeders (17 and 8 ng Hg g^{-1} d.w. respectively) while it is very similar for deposit feeders (22 and 35 ng Hg g^{-1} d.w. respectively), filter feeders (28 and 39 ng Hg g^{-1} d.w. respectively), and generalist feeders (26 and 40 ng Hg g^{-1} d.w. respectively). MeHg is notably higher for predators and highest for top predators in the observations with 77 and 381 ng Hg g^{-1} d.w. respectively which is close to the 54 and 337 in the AS model for predator and top predator than the 49 and 73 ng Hg g^{-1} in the base model respectively.

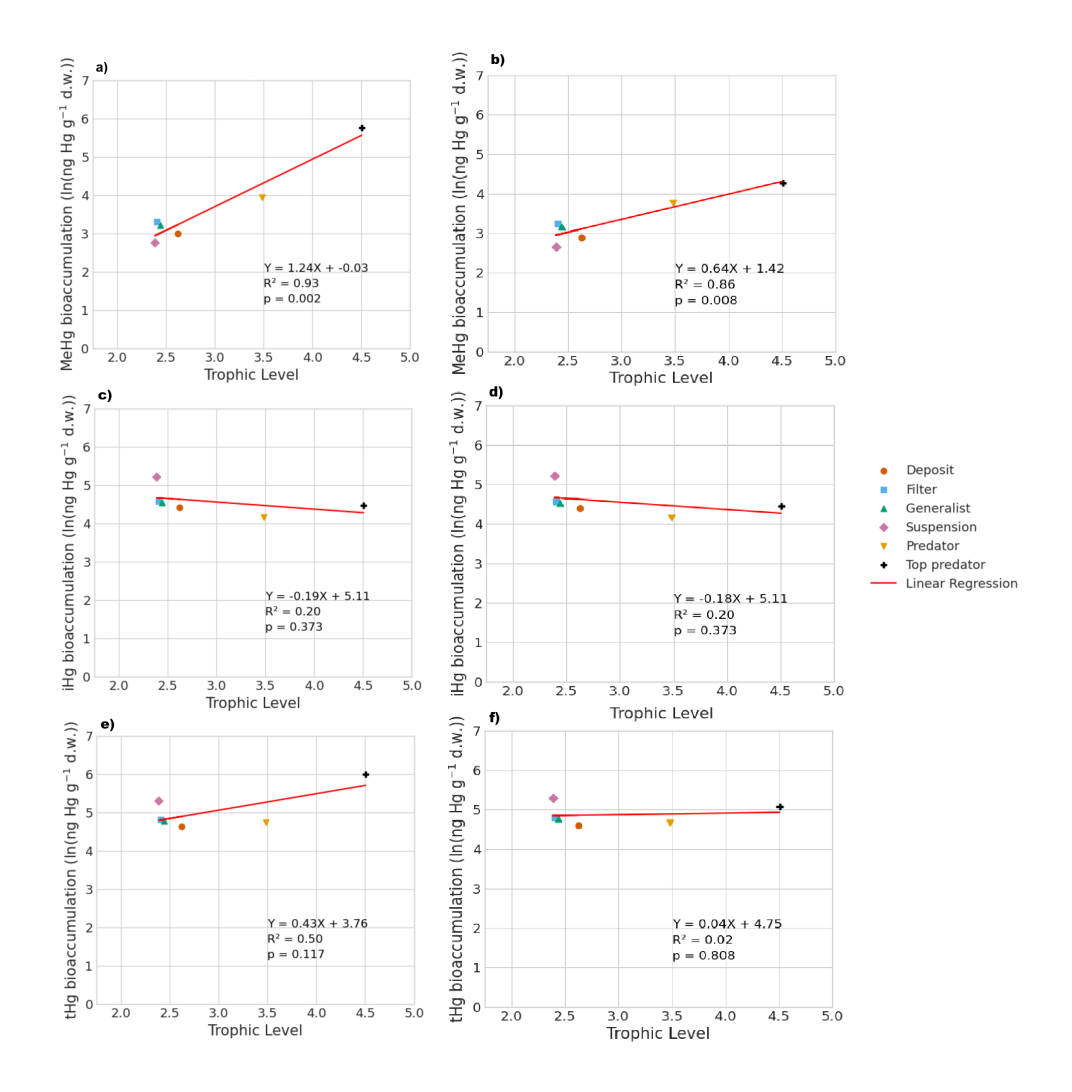


Figure 4. The influence of trophic level on the bioaccumulation of MeHg, iHg, and tHg in both the AS (panels a, c, e) and the base model (panels b, d, f). In the AS model, the relationship with trophic level is stronger, where ln(MeHg)=1.24TL-0.03, compared to the base model, which is ln(MeHg)=0.64TL+1.42. TL represents trophic level, and MeHg is expressed in ng Hg g⁻¹ d.w. For iHg, the bioaccumulation patterns are nearly identical, with ln(MeHg)=-0.19TL+5.11 for the AS model and ln(MeHg)=-0.18TL+5.11 for the base model, both showing a weak inverse correlation with trophic level, largely due to higher iHg levels in low trophic level feeders. In terms of tHg, there is a higher increase in bioaccumulation in the AS model (ln(MeHg)=0.43TL+3.76) compared to the base model (ln(MeHg)=0.04TL+4.175), driven by the stronger association between MeHg and trophic level in the AS model.

Table 3. Statistical analysis of model performance for iHg and MeHg levels by feeding strategy for Southern North Sea (SNS) and Northern North Sea (NNS). The predator and top predator of both the default setup and Allometric Scaling (AS) model is shown. For all individual feeding strategies the normalised bias is shown, and for the full model the RMSE, NRMSE, R²_{Pearseon}, and R²_{Residual} is shown.

	s	NS	NNS		
	iHg	МеНд	iHg	MeHg	
Suspension	0.18	1.09	-0.18	0.24	
Filter	1.48	-0.28	1.45	-0.69	
Deposit	1.01	-0.36	0.34	-0.75	
Generalist	1.31	-0.35	1.23	-0.73	
Predator	0.41	-0.37	0.07	-0.77	
Top predator	-0.22	-0.80	-0.46	-0.92	
Predator (AS)	0.41	-0.31	0.07	-0.75	
Top predator (AS)	-0.22	-0.12	-0.46	-0.67	
Overall Model Perfo	ormance				
RMSE	40	132	40	146	
NRMSE	0.36	0.35	0.35	0.39	
$R^2_{Pearson}$	0.61	0.86	0.24	0.94	
$R^2_{Residual}$	<0	<0	<0	<0	
RMSE (AS)	40	22.8	40	108	
NRMSE (AS)	0.36	0.061	0.35	0.29	
R ² Pearson (AS)	0.61	>0.99	0.24	0.99	
R ² _{Residual} (AS)	<0	0.96	<0	<0	

3.5.2 The statistical performance of the model

355

360

Our model estimates that suspension feeders have the highest iHg values, which is in line with observations. In our model, the high iHg values are caused by the very efficient Hg scavenging of small DOM particles. These small particles have the highest Hg/C ratio (as was shown in Fig. 3) and can only be consumed by suspension feeders. This leads to very high iHg and low MeHg in suspension feeders. The result that our model partially replicates the high iHg values in the suspension feeders indicates that we underestimated this effect or that additional factors were contributing to the high iHg levels found. In Orani et al. (2020), it is demonstrated that the extremely low MeHg/Hg ratio in suspension-feeding sponges may be caused by the demethylation of MeHg by symbiotic bacteria. Our study expands on this by showing that the high iHg and low MeHg values can partially be explained by the consumption of DOM by suspension feeders, but the proposed demethylation could explain why we cannot fully replicate the observations. Based on this, it is likely that the unique bioaccumulation values in suspension feeders are caused by a combination of their ability to feed on DOM, together with biochemical processes that occur in their

Table 4. Comparison of modeled and observed Hg and MeHg bioaccumulation in different feeding strategies for the Southern North Sea (SNS), Northern North Sea (NNS), and field observations. Values are presented as ranges with means in parentheses. Units are ng Hg g d.w. for iHg and MeHg, and% for MeHg percentage. The bottom two rows are the predator and top predator from the AS model (AS).

	l I	Model (SNS)		Model (NNS)		Observations			
	iHg	МеНд	% MeHg	iHg	МеНд	% MeHg	iHg	МеНд	% MeHg
Suspension	141-213 (180)	14-20 (17)	9	72-186 (125)	6-14 (10)	7	58-515 (152)	1-26 (8)	5
Filter	85-109 (97)	23-32 (28)	22	80-120 (96)	10-15 (12)	11	3-82 (39)	2-173 (39)	50
Deposit	73-93 (83)	19-26 (22)	21	41-71 (55)	7-12 (9)	14	9-113 (41)	2-231 (35)	46
Generalist	82-105 (94)	21-29 (26)	22	71-114 (90)	8-13 (11)	11	3-113 (40)	2-231 (40)	50
Predator	62-67 (65)	47-50 (49)	43	45-51 (49)	16-19 (18)	27	9-329 (46)	4-367 (77)	63
Top predator	83-91 (88)	69-76 (73)	45	51-71 (61)	26-39 (32)	34	69-266 (113)	77-895 (381)	77
Predator (AS)	45-48 (47)	52-55 (54)	54	45-51 (49)	18-20 (19)	28	9-329 (46)	4-367 (77)	63
Top predator (AS)	62-66 (64)	320-348 (337)	84	51-71 (61)	109-147 (127)	68	69-266 (113)	77-895 (381)	77

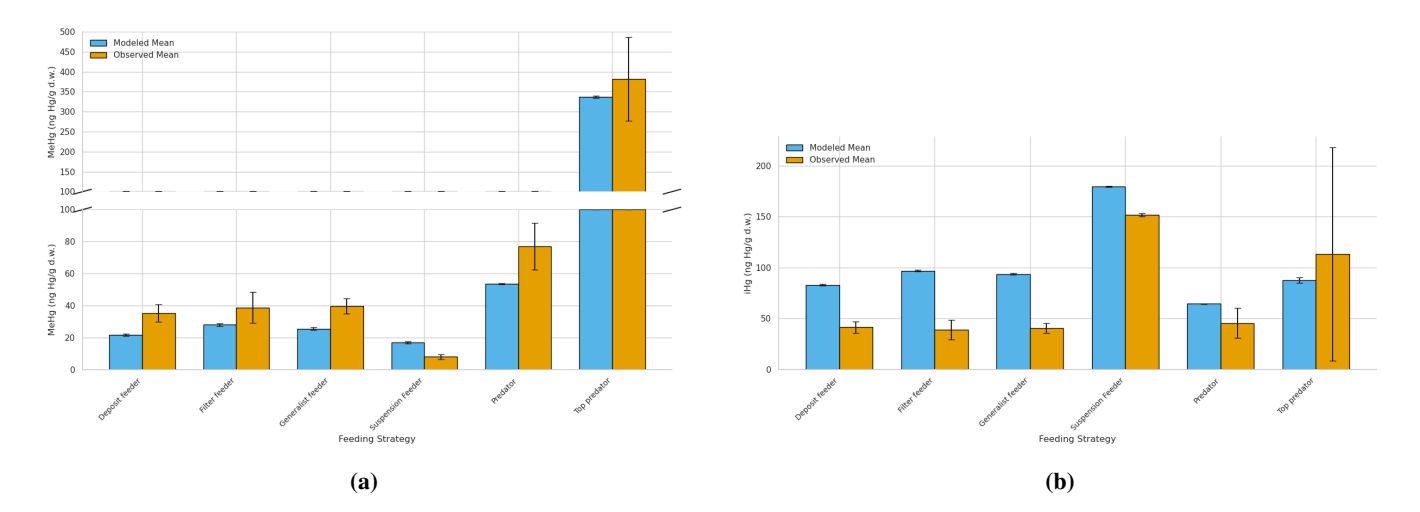


Figure 5. Comparison of bioaccumulation across feeding strategies between the Southern North Sea AS model and observations. The bars represent the mean with the error bar showing 1SE. Figure 5a) shows MeHg bioaccumulation. Notably is that Top predators show the highest levels, followed by predators, with generalists and filter feeders at intermediate levels and deposit feeders at lower levels. Suspension feeders have the lowest MeHg. 5b) shows iHg Bioaccumulation. Suspension feeders show increased iHg, while all other categories except top predators are overestimated by the model. Top predators have high observed iHg not fully captured by the model.

symbiotic bacteria. Notably, while not statistically significant, our model overestimates the mean iHg values with a normalized bias of 0.61 and 0.77 for filter feeders and 0.60 and 0.60 for generalist feeders in the Southern North Sea and Northern North Sea, respectively. In Fig 3 we see that the majority of this iHg originates from bioconcentration. This discrepancy is described in more detail later in the paper.

The $R^2_{Pearson}$ is high (>0.86) for MeHg in all setups and exceeds 0.99 in the AS model, indicating that the model captures the relative differences between feeding strategies well. For iHg, performance is lower, particularly in the Northern North Sea ($R^2_{Pearson} = 0.24$). The ability to reproduce absolute bioaccumulation is more limited. Only the AS model in the Southern North Sea shows good agreement ($R^2_{Residual} = 0.96$), while all other setups yield $R^2_{Residual} < 0$, suggesting that using the mean of the observations would outperform the model.

This can be explained, as baseline MeHg levels vary between sampling regions. Notably, the AS model in the Southern North Sea performs well both in reproducing overall MeHg levels and in explaining variability across feeding strategies. Even when excluding predators and top predators, $R^2_{Pearson}$ remains high (0.80), suggesting that feeding strategy effects are captured across trophic levels and are not just driven by high MeHg levels in predatorial feeding strategies. In contrast, the Northern North Sea has a high $R^2_{Pearson}$ (=0.94) but low $R^2_{Residual}$ (<0) so it captures the effect of feeding strategies while not being able to replicate absolute MeHg concentrations.

3.5.3 The effect of water column mixing

375

380

385

390

395

Finally, if we compare our 2 setups, we find that our model predicts MeHg bioaccumulation three times higher in the shallow permanently mixed Southern North Sea setup than in the deeper seasonally mixed Northern North Sea setup. In our model, this is mostly caused because the megabenthos in the shallow Southern North Sea can feed directly from the phyto- and zooplankton bloom. This gives them greater access to protein-rich food that strongly binds to MeHg. In the Northern North Sea, the ecosystem revolves around the sinking of detritus. Since detritus binds less MeHg than living material, there is a reduction in overall Hg bioaccumulation in the Northern North Sea compared to the Southern North Sea, but especially for MeHg. This means two things. First of all, in the well-mixed Southern North Sea, filter feeders have a competitive advantage as they can filter out fresh food and feed on relatively high trophic level zooplankton. Filter feeders have the highest MeHg values at the base of the benthic food web, and therefore a higher concentration of filter feeders will lead to a higher fraction of filter feeders in the predator diet and thus more MeHg. Additionally, since the filter feeders feed on living pelagic material with higher MeHg values, the filter feeders themselves also have higher MeHg. Thus, predators and, consequently, the top predators have higher MeHg values in the Southern North Sea compared to the Northern North Sea as a result of the increased water column mixing. In Fig. 6 we show the correlation between the natural logarithm of bioaccumulated Hg and the trophic level in the Northern North Sea. Interestingly, the trophic level of megabenthos is higher in the Northern North Sea, while the bioaccumulation level is lower. This is because the detritus is cycled more often in the pelagic before it is consumed by megabenthos; because the detritus is in constant equilibrium with the water column for its partitioning of Hg and MeHg, this does not translate to higher bioaccumulation. This lower bioaccumulation results in lower concentrations of MeHg in high trophic levels of fish.

3.6 The role of the feeding strategy on MeHg bioaccumulation in a single case study

In addition to using the global bioaccumulation dataset to evaluate our hypothesis that the feeding strategy is a key driver of 400 bioaccumulation, we also evaluate if our hypothesis holds true when analyzing a comprehensive published dataset from a single

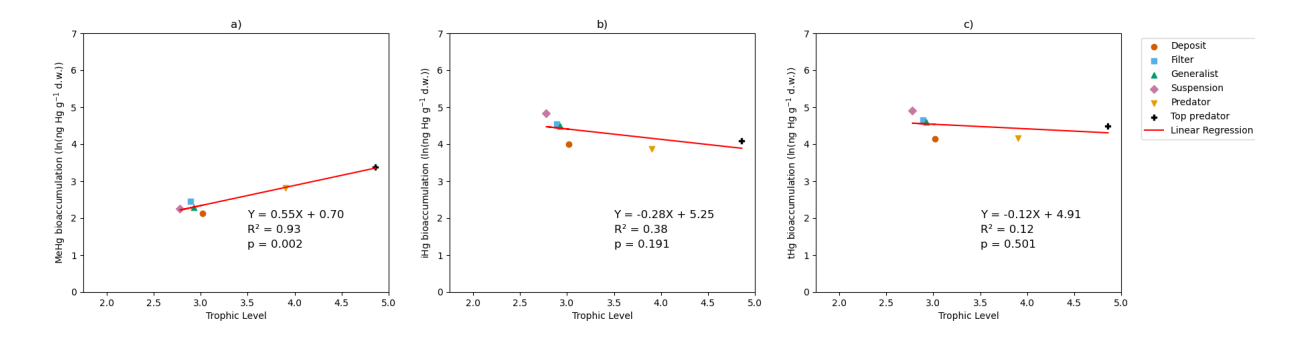


Figure 6. The natural logarithm of bioaccumulation for a) MeHg, b) iHg, and c) tHg in the permanently mixed Northern North Sea model shows that while the slope for MeHg bioaccumulation is comparable in the Northern and Southern North Sea with a slope of 0.55 and 0.64 respectively, its overall level of MeHg bioaccumulation is lower than in the Southern North Sea. Similar as in the Southern North Sea, there's no significant correlation between trophic level and iHg bioaccumulation.

study. The fit of the linear model against the natural logarithm of the bioaccumulated MeHg based on the data published by Mc-Clelland et al. (2024) is shown in Fig. 7. The R² is similar with 0.43 and 0.45 in the CB and MT respectively, while the bioaccumulation is a bit lower in the CB (log(MeHg_{BA})=0.137+1.14*TL) compared to that in the MT (log(MeHg_{BA})=0.256+1.39*TL), where MeHg_{BA} is the bioaccumulated MeHg in ng Hg mg⁻¹ d.w. and TL is the trophic level. The influence of the feeding strategy on MeHg bioaccumulation based on the results of McClelland et al. (2024) is shown in Table 5. While the only significant effect is deposit feeders in the MT having less MeHg than would be expected on their trophic positions, some other effects are consistent, albeit not significant in both locations. The strongest effect is that filter feeders have consistently higher MeHg (residuals are 0.7 in the CB and 0.8 in the MT), while deposit feeders have lower MeHg (residuals are -0.2 in the CB and -0.5 in the MT). The results of the same analyses for phyla are shown in Table 6. Here we see two consistent significant effects, Molluscs have elevated MeHg levels (residuals are 0.61 in the CB and 0.51 in the MT) while arthropods have reduced MeHg values (residuals are -0.35 in the CB and -0.30 in the MT). The percentage difference in MeHg bioaccumulation per feeding strategy is visualised in Fig. 8 and per phyla in Fig. 9. The average percentage difference between observed and the expectation based on trophic level is 102% and 128% in the CB and MT respectively for filter feeders, while deposit feeders have 19 and 37% less MeHg than would be predicted based on trophic level alone in the CB and MT respectively. In the analysis per phylum, we see that molluscs have highly elevated MeHg levels with an increase of 66% and 85% respectively in the CB and MT. The largest reduction in observed MeHg compared to the predicted values based on trophic level is in arthropods; here there is a decrease compared to the predicted values of 29% and 26% in the CB and MT respectively.

405

410

415

The results of the final analyses are shown in Table 7. Despite the lower sample size, which reduces statistical power, the results indicate that filter feeders consistently have higher MeHg levels than predicted based on their trophic position and phyla, while deposit feeders tend to have lower MeHg concentrations. These results are stronger in the MT with a change of 118% and -40% in filter and deposit feeders respectively than in the CB with a change of 7.2% and -14.8% in filter and deposit

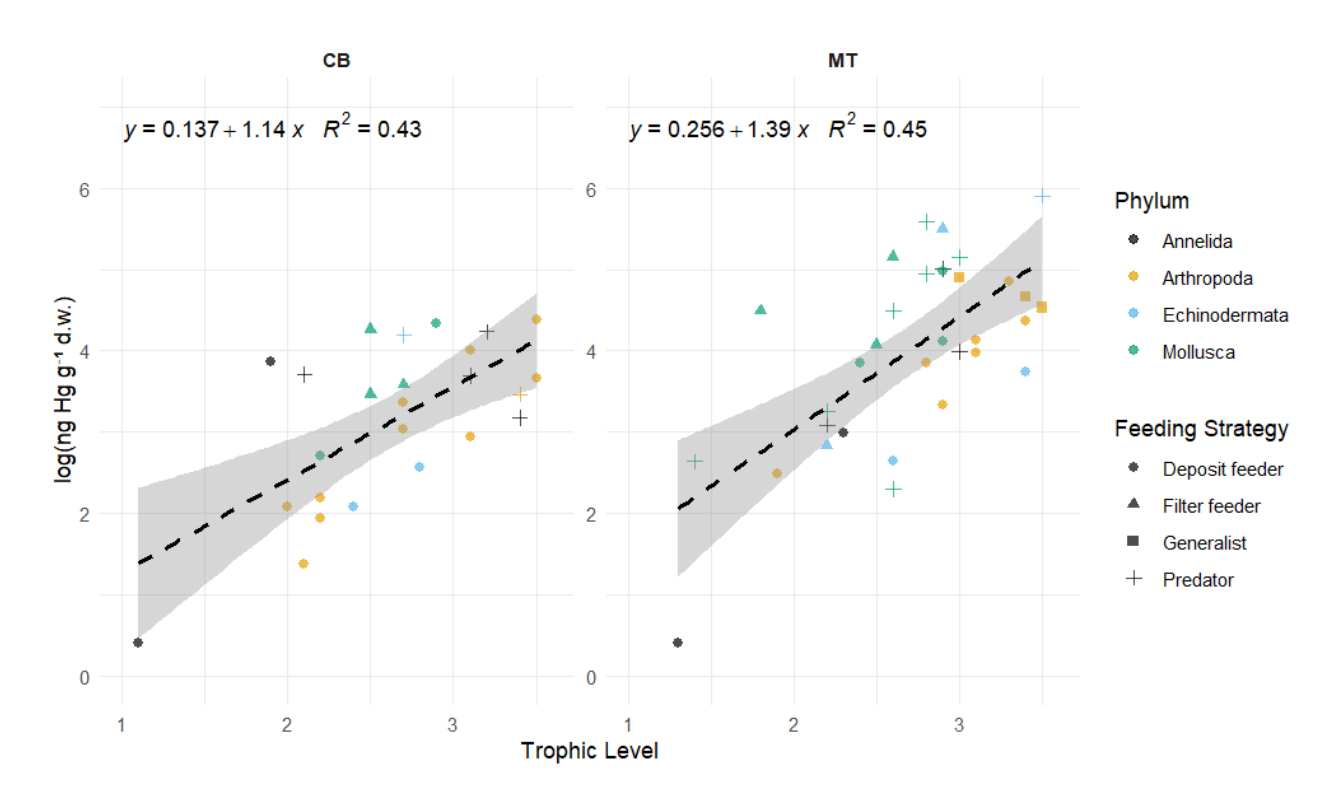


Figure 7. The linear fitted model between the natural logarithm of the bioaccumulated MeHg in ng Hg mg⁻¹ d.w. and the Trophic Level in the data presented by McClelland et al. (2024). For extra clarity the different Phyla shown with different colors while the different feeding strategies are marked with different symbols. In both the CB and MT setups there positive relationship between trophic level and the bioaccumulation of MeHg, but R² is only 0.43 and 0.45 in the CB and MT respectively, so it does not explain the full variation in bioaccumulation.

Table 5. Mean residuals (\pm SE) of log(MeHg) by feeding strategy and region, after trophic level correction. Significant deviations (p < 0.05) are marked with *.

Region	Feeding Strategy	n	Mean Residual \pm SE	p-value
СВ	Deposit feeder	16	-0.208 ± 0.181	0.268
CB	Filter feeder	3	0.704 ± 0.286	0.133
CB	Predator	6	0.203 ± 0.331	0.568
MT	Deposit feeder	15	-0.467 ± 0.159	0.011^{*}
MT	Filter feeder	5	0.824 ± 0.395	0.105
MT	Generalist	3	-0.143 ± 0.319	0.698
MT	Predator	12	0.277 ± 0.226	0.247

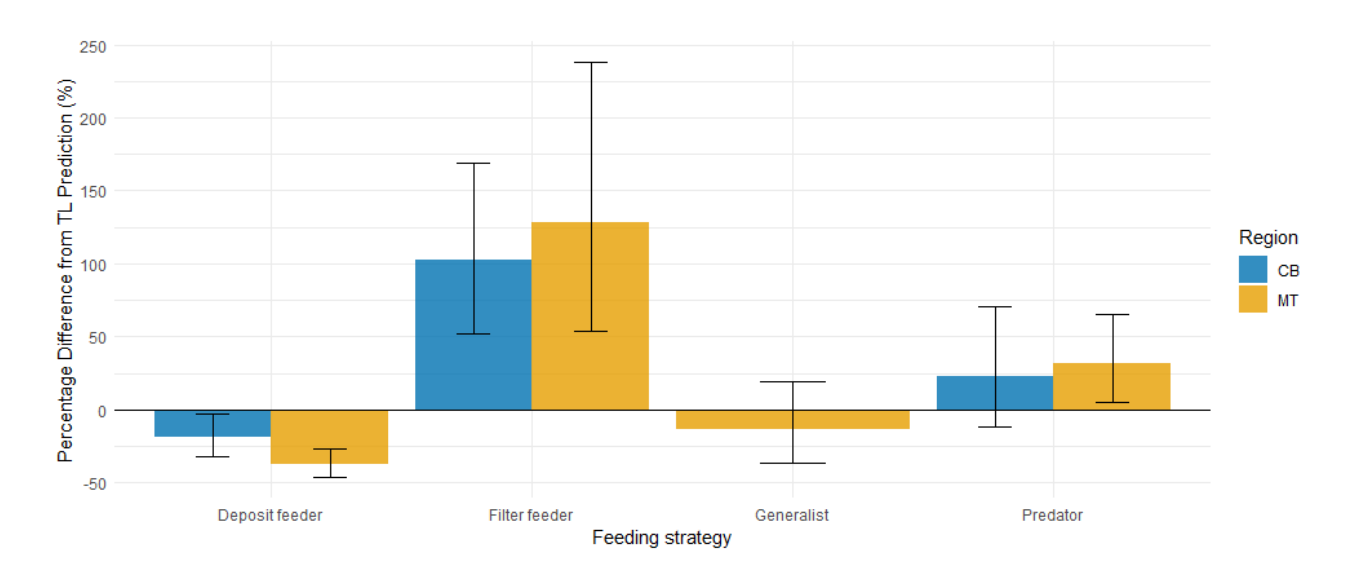


Figure 8. Percentage difference from trophic level predicted MeHg concentrations by feeding strategy, with error bars showing ± 1 SE. In both CB and MT regions, filter feeders have elevated MeHg levels relative to trophic level based expectations, while deposit feeders are reduced. Predators display higher MeHg than predicted, though the effect is smaller than in filter feeders; in CB, this increase does not exceed one SE. Generalist feeders have a slight reduction compared to expectations, but this is well within one SE, and were not present in CB for cross-region comparison.

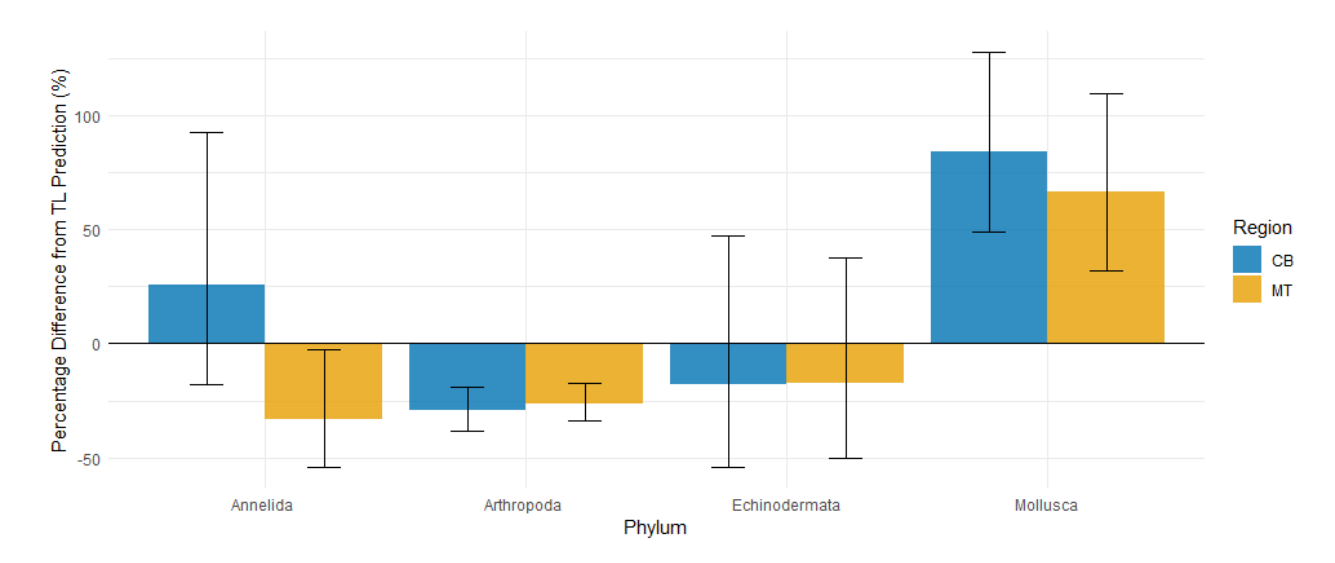


Figure 9. Percentage difference from the predicted MeHg bioaccumulated based on trophic level per phyla, the error bars represent ± 1 SE. The notable phyla are Mollusca and Arthropoda, while Mollusca have a notable increase in MeHg bioaccumulation compared to the prediction of 85% and 66% respectively in the CB and MT, there is a reduction of 26% and 29% in Arthropoda in the CB and MT respectively. Annelida are inconsistent with an increase in the CB and decrease in the MT compared to the predictions. Echinodermata have a mean reduction compared to the prediction in both the CB and the MT, but the SE is much larger than the mean effect.

Table 6. Mean residuals (\pm SE) of log(MeHg) by phylum and region, after trophic level correction. Significant deviations (p < 0.05) are marked with *.

Region	Phylum	n	Mean Residual \pm SE	p-value
СВ	Annelida	6	0.229 ± 0.424	0.612
CB	Arthropoda	11	-0.349 ± 0.137	0.0294*
CB	Echinodermata	3	-0.198 ± 0.584	0.767
CB	Mollusca	5	0.611 ± 0.211	0.0446*
MT	Annelida	5	-0.405 ± 0.377	0.343
MT	Arthropoda	12	-0.304 ± 0.111	0.0196*
MT	Echinodermata	5	-0.188 ± 0.509	0.730
MT	Mollusca	13	0.509 ± 0.231	0.0482^{*}

feeders respectively. It must be stated that this final analysis is included to address potential concern between the co-correlation of phyla and feeding strategy, but the problem of the reduced sample size has to be addressed. In the CB, where the increase in MeHg in filter feeders is rather low after correcting for both trophic level and feeding strategy, there are only three filter feeders, which are molluscs, and they make up 3/5 mollusc samples in this location, meaning that results should be seen with skepticism as filter feeders and molluscs have too much overlap. On the other hand, in the MT, there are five filter feeders from multiple phyla (Mollusca and Echinodermata) and the effect is considerably stronger with filter feeders having 118% more MeHg than would be expected based on their trophic level and phyla.

Table 7. The effect of feeding strategy on MeHg bioaccumulation per Region compared to the prediction accounting for both trophic level and feeding strategy. Significant (p < 0.05) is marked with *. There is still a consistent increase in filter feeders and a consistent decrease in deposit feeders. This is effect is larger in the MT with a relative percentage increase of 118% in filter feeders and a decrease of 40% in deposit feeders.

Feeding Strategy	% Diff (MT)	p-value (MT)	% Diff (CB)	p-value (CB)
Deposit feeder	-40.0	0.034*	-14.8	0.888
Filter feeder	118.0	0.034*	7.2	0.888
Generalist	-25.9	0.563	-	_
Predator	3.0	0.895	9.4	0.888

430 4 Discussion

4.1 The role of feeding strategy on the bioaccumulation of MeHg

Overall we find that the feeding strategy plays an important role in the bioaccumulation of MeHg in our model, the global dataset, and the single dataset published by McClelland et al. (2024). Because of this, we find it convincing that the role of the feeding strategy in MeHg bioaccumulation deserves further attention in both modeling and empirical studies.

435 **4.2** The AS model

440

450

455

460

Our base model fails to reproduce the high values in the top predators, but this is improved in the AS model. The normalized bias is reduced from -0.80 to -0.22. In the AS model, we get a linear relationship of 1.24x-0.03 (R²=0.93), which has a similar slope to the 1.14x+0.387 and 1.39+0.256 found in CB and MT station of the McClelland et al. (2024) dataset respectively. The improvement in the AS model compared to the base model indicates that the lower MeHg release rates in high-trophic-level animals should be taken into account. We tried to run the model with the lower MeHg release rate in all megabenthos, but this resulted in unrealistically high values in both the base and top of the food web, so we cannot just use the lower MeHg release rate at every trophic level. Because of this, we conclude that in addition to the feeding strategy, the difference in the release rate of MeHg related to body size, metabolic rate, or activity also likely has a significant contribution to the high MeHg values in high-trophic-level animals.

445 4.3 Bioconcentration of iHg

The largest bias in our model, which remains uncorrected in the AS model, is the overestimation of iHg in the filter and generalist feeders. Although the modeled iHg values are not out of the observed range, the consistently high normalized bias indicates that the model overestimates the bioaccumulation of iHg. In Fig. 3 we can see that the vast majority of iHg in filter and generalist feeders originates from bioconcentration. The most important driver of bioconcentration is the ratio between uptake and release rate, or the uptake-release ratio. Our model has an uptake-release ratio of 2101 g⁻¹ d.w. This is derived from Tsui and Wang (2004), as it represents the lowest ratio found in the literature. The exact rate was obtained by withdrawing the modeled carbon excretion rate and deducting this from the measured iHg release rate to have an iHg-specific release rate; this rate was found to be 0.04 d⁻¹, as presented in Amptmeijer et al. (2025). Other studies such as Pan and Wang (2011) found higher uptake-release ratios between 424 and 781 l g⁻¹ d.w.

The discrepancy between the modeled and observed iHg can be caused by several factors. First, iHg concentrations in North Sea megabenthos could be higher than those reported in other coastal zones. However, there are no empirical data to support or invalidate this conclusion at the moment. Secondly, translating experimentally obtained uptake and release rates to observations of iHg might depend on the drivers that are not captured in the model. In either case, it is hard to verify the root of this high normalized bias, as the bioaccumulation of iHg is comparatively understudied compared to the bioaccumulation of MeHg, both in models and empirical studies.

4.4 Model structural limitations

465

470

485

490

The GOTM-MERCY-ECOSMO coupled system captures the influence of feeding strategy on MeHg bioaccumulation, but performance differs between regions. The Southern North Sea setup performs well in pelagic Hg cycling and benthic bioaccumulation, whereas the Northern North Sea setup underestimates MeHg in all benthic groups and shows unexpectedly high mesozooplankton tHg, which cannot be validated due to a lack of data. The model predicts lower MeHg bioaccumulation in deeper water, which is not true for the observations by McClelland et al. (2024). This suggests that MeHg fluxes from the pelagic to the benthic system are underestimated. In shallow waters, megabenthos can feed directly on the phytoplankton and zooplankton blooms, which leads to a strong bentho-pelagic exchange of organic carbon and Hg. In deeper waters, megabenthos mainly rely on detritus that sinks from the euphotic, which, in our model, carries less MeHg. But the higher performance in shallow conditions combined with the reduced performance in deeper conditions indicates that the model could be improved in areas driving deep water MeHg bioaccumulation, such as sediment Hg chemistry, deep-water Hg speciation, the bentho-pelagic coupling, or the transport of Hg to deeper water due to the sinking of organic material.

4.5 Data-related limitations

Combining the results of the model and the literature studies is difficult due to the high uncertainty in most drivers, including
the organic material content of dry weight, and the result should be viewed with skepticism. For example, the data analyses by
McClelland et al. (2024) were prepared to mimic consumption by predators: for small arthropods, their skin was not removed,
but for gastropods and bivalves, the shell was not taken into account for the weight as predators would typically not eat this.
The concentration of MeHg per unit energy is arguably the key measure in bioaccumulation. Predators need to ingest a specific
energy amount, so if a prey is composed of half organic material and half non-organic components, such as shell, its MeHg
content per dry weight is halved. However, predators would consume double the dry weight to obtain the energy, and thus the
same MeHg. In general, the energy appears to be consistent with Ash Free Dry Weight (AFDW), as such ideally we would
normalize all measurements of MeHg bioaccumulation per AFDW (Weil et al., 2019).

Unfortunately, doing this conversion reliably on published data is not possible as AFDW varies with the age and body size of animals, which information is not always registered and made available (Eklöf et al., 2017).

4.6 Potential improvements

The model has the same rates for all megabenthos groups. This allows us to isolate the effect of the feeding strategy, but it should be taken into account that this also means that the model is limited in its ability to predict bioaccumulation of iHg or MeHg in specific animals. Our model is run in the North Sea, while most of the field observations are from different regions. This means that this study should be seen as a hypothesis-generating work that identifies the role of feeding strategies on the bioaccumulation of iHg and MeHg as a potential direction for further empirical studies, rather than a complete classification. Based on this work, however, it appears that the inclusion of megabenthos with different feeding strategies could improve

the performance of MeHg bioaccumulation models. At the same time, our analyses demonstrate the underperformance of the model in simulating the deep water bentho-pelagic coupling, which indicates that the performance of the ECOSMO E2E-MERCY-GOTM coupled system should be critically evaluated before it can be used for predictive bioaccumulation modelling in deeper water.

5 Summary and conclusion

500

505

515

520

In this study, we analyze the role of the trophic level and the feeding strategy on the bioaccumulation of iHg and MeHg. We did this by performing a literature study and running a fully coupled 1D model in two idealized setups representing two different hydrodynamic regimes in which megabenthic communities can live. Our study estimates that the trophic level predicts up to 32% of the variability of MeHg in the benthic food web. If we include both the feeding strategy and the trophic level, this increases to 72%. We show that several feeding strategies have significant differences.

We show that there are notable differences between feeding strategies. iHg is higher in suspension feeders and MeHg is low in suspension feeders and grazers, while filter feeders have the highest MeHg followed by deposit feeders. Our model expands on this by demonstrating that we can accurately model the bioaccumulation of iHg and MeHg at the base of the food web by only taking the feeding strategy into account.

We find it convincing that both our model results, the literature study in which we aggregate all measurements, and the literature study where we take samples from a single study all suggest similar patterns where feeding strategy is an important driver of bioaccumulation at the base of the food web, even if these results should be seen with skepticism due to the large uncertainty in the model. Because feeding strategy in our base model correlates well with observed iHg (R²=0.61) and MeHg $(R^2=0.86)$ in the Southern North Sea setup, it appears that the feeding strategy is a key driver controlling the bioaccumulation of both iHg and MeHg at the base of the food web. However, this strong performance is mostly because 4 out of our 6 megabenthos groups are low trophic level non-predators, and our base model starts to underperform considerably in its ability to model MeHg bioaccumulation in higher trophic levels. This problem is solved by taking into account the allometric scaling law and assuming that MeHg removal from the organism is not linked to the total but rather to the base metabolic rate. Because of this, we accept our hypothesis that the feeding strategy is an essential driver of the bioaccumulation of iHg and MeHg in low-trophic-level animals, but other differences in the organisms between high- and low-trophic-level animals should also be taken into account when predicting MeHg values in high-trophic-level fish. Our model and observation focus on lowertrophic-level benthic invertebrates, with some high-trophic-level animals added to create context. The importance of this for the bioaccumulation of MeHg in animals of high trophic levels is that all biomagnification is an exponential function starting at the base of the food web. Therefore, a change in MeHg at the base of the food web will correspond to a similar relative increase at the top of the food chain. Because the feeding strategy has such a large impact on the base of the food web, high trophic-level animals could have considerably different MeHg values depending on the species composition of the base of the food web.

Interestingly, despite the lower biomagnification potential of iHg, its high abundance in certain low-trophic-level animals can lead to higher tHg in low-trophic-level animals than in higher-trophic-level animals. This discrepancy can distort risk perception, as safety assessments often rely on tHg measurements that do not distinguish between iHg and MeHg. Animals, such as suspension-feeding bivalves, may have high Hg values while remaining safe for human consumption. Our findings demonstrate the importance of Hg speciation data in marine organisms to help improve food safety guidelines and inform regulatory policies.

5.1 Societal relevance & future work

535

540

545

550

555

Our study highlights the critical role of benthic diversity in driving MeHg bioaccumulation. Both trophic interactions and the feeding strategy significantly influence MeHg bioaccumulation, which has important implications for seafood safety and fisheries management. Understanding these processes can help explain the spatial and temporal variability in the MeHg content of fish, which is crucial for policymakers to develop effective regulations that safeguard human health and marine ecosystems.

Filter feeders and molluscs typically accumulate more MeHg than other organisms at similar trophic levels. This pattern is consistent not only in our models but also in available data. This raises a hypothesis that expanding bivalve populations, as seen in mussel or oyster farming, might affect MeHg bioaccumulation in higher trophic levels. This is supported by the observations that fish in lakes invaded by zebra mussels have higher Hg levels than fish in lakes without zebra mussels Blinick et al. (2024). However, such ecological alterations also impact other bioaccumulation factors like biomass distribution and trophic interactions. While our findings support the role of filter feeders and molluscs in MeHg dynamics and higher bioaccumulation in top predators, the complexity of ecological situations requires further case-specific studies to understand if and when bivalve communities lead to increased MeHg transfer.

Modeling studies can help our understanding of the factors influencing MeHg bioaccumulation, but the ability to accurately predict MeHg bioaccumulation needs to be carefully validated. Our findings reveal that filter-feeding molluses and DOM-utilizing suspension feeders have different Hg bioaccumulation patterns compared to other megabenthos. Modeling bivalve aquaculture or DOM-consuming suspension feeders can help explore their potential role in altering MeHg bioaccumulation. Understanding how functional traits like feeding strategy influence MeHg transfer remains key to improving both predictive models and environmental risk assessments.

Our findings suggest that fish from food webs dominated by filter feeders would have the highest MeHg content, since filter feeders have the highest MeHg content in both our model and observations. It also creates an indication that the introduction of bivalve communities in the form of mussel or oyster farming could increase MeHg levels in higher food chains. However, such changes in the ecosystem would inevitably change other factors in the ecosystem, including biomass and trophic interactions that are also essential drivers for MeHg bioaccumulation. While our model should be seen as a hypothesis-generating work that requires empirical validation, it does suggest that case-by-case studies are needed to fully understand how changes in the base of the food web will affect the concentration of MeHg in high trophic level fish.

Based on our results, we strongly recommend targeted field studies that systematically measure iHg, MeHg, and trophic levels in diverse marine communities to assess how the structure of the food web influences the bioaccumulation of MeHg in seafood.

560 6 Acknowledgments

Readability suggestions for this paper were generated using rAI tools such as ChatGPT (OpenAI), while AI-based spell checks such as Grammarly and Writefull were used to correct spelling. In addition, AI tools helped optimize the R and Python scripts and provide coding suggestions. All suggestions were implemented only after critical manual evaluation. Finally, Google Scholar and Perplexity were used to find sources for literature research, which were consequently manually read, verified, and cited.

Author contributions

565

The contributions per author are listed in Table 8.

Table 8. Contributions per Author. Authors are: David Johannes Amptmeijer (DA), Andrea Padilla (AP), Sofia Modesti (SM), Prof. Dr. Corinna Schrum (CS), and Dr. Johannes Bieser (JB).

Contributor role	Role definition	Authors
Conceptualisation	Conceptualized the study	DA, JB, CS
Conceptualisation	Developed the research objectives	DA, JB, CS
Methodology	Implementation of the model into FABM	DA
Wellodology	Compiled the database of megabenthos iHg and MeHg obser-	DA, AP
	vations	
Evaluation	Evaluated the model performance against observations	JB, DA, AP, SM
Z, uzuution	Performed statistical tests on the observations	DA, AP, SM
Writing	Writing of the original draft	DA
Willing	Review of the original draft and quality control	AP, SM, JB, DA
Supervision	Supervised the development of the work	CS, JB, DA
Funding acquisition	Acquired funding via the GMOS-Train ITN	JB

Conflict of interest

None of the authors declare any conflict of interest.

570 Funding

This research has been funded by the European Union's Horizon 2020 research and innovation programme under the Marie Sklodowska-Curie grant agreement no. 860497.

References

- Allison, J. D., Allison, T. L., and Ambrose, R. B.: Partition coefficients for metals in surface water, soil, and waste. U.S. Environmental Protection Agency, Washington, DC,, Tech. rep., www.epa.gov/athens/wwqtsc, 2005.
 - Amptmeijer, D. J., Bieser, J., Mikheeva, E., Daewel, U., and Schrum, C.: Bioaccumulation as a driver of high MeHg in coastal Seas, EGUsphere [preprint], https://doi.org/10.5194/egusphere-2025-1486,2025., 2025.
 - Bieser, J., Amptmeijer, D., Daewel, U., Kuss, J., Soerenson, A. L., and Schrum, C.: The 3D biogeochemical marine mercury cycling model MERCY v2.0; linking atmospheric Hg to methyl mercury in fish, Geoscientific Model Development Discussions, pp. 1–59, https://doi.org/10.5194/GMD-2021-427, 2023.
 - Blinick, N. S., Link, D., Ahrenstorff, T. D., Bethke, B. J., Fleishman, A. B., Janssen, S. E., Krabbenhoft, D. P., Nelson, J. K. R., Rantala, H. M., Rude, C. L., and Hansen, G. J. A.: Increased mercury concentrations in walleye and yellow perch in lakes invaded by zebra mussels, https://doi.org/10.1016/j.scitotenv.2024.177515, 2024.
- Bolding, K., Bruggeman, J., Burchard, H., and Umlauf, L.: General Ocean Turbulence Model GOTM, https://doi.org/10.5281/ZENODO.4896611, 2021.
 - Bruggeman, J. and Bolding, K.: A general framework for aquatic biogeochemical models, Environmental Modelling & Software, 61, 249–265, https://doi.org/10.1016/J.ENVSOFT.2014.04.002, 2014.
 - Burchard, H., Bolding, K., and Villarreal, M. R.: GOTM, a General Ocean Turbulence Model. Theory, implementation and test cases, Tech. rep., 1999.
- 590 Campanella Id, F., Auster, P. J., Taylor, J. C., and Muñoz, R. C.: Dynamics of predator-prey habitat use and behavioral interactions over diel periods at sub-tropical reefs, PLOS ONE, 2, https://doi.org/10.1371/journal.pone.0211886, 2019.
 - Chakravarti, L. J. and Cotton, P. A.: The Effects of a Competitor on the Foraging Behaviour of the Shore Crab Carcinus maenas, PLoS ONE, 9, 93 546, https://doi.org/10.1371/journal.pone.0093546, 2014.
- Cibic, T., Baldassarre, L., Cerino, F., Comici, C., Fornasaro, D., Kralj, M., and Giani, M.: Benthic and Pelagic Contributions to

 Primary Production: Experimental Insights From the Gulf of Trieste (Northern Adriatic Sea), Frontiers in Marine Science, 9,

 https://doi.org/10.3389/fmars.2022.877935, 2022.
 - Coquery, M. and Cossa, D.: Mercury speciation in surface waters of the north sea, Netherlands Journal of Sea Research, 34, 245–257, https://doi.org/10.1016/0077-7579(95)90035-7, 1995.
- da Silva, J. K. L., Garcia, G. J., and Barbosa, L. A.: Allometric scaling laws of metabolism, Physics of Life Reviews, 3, 229–261, https://doi.org/10.1016/J.PLREV.2006.08.001, 2006.
 - Daan, R. and Mulder, M.: The macrobenthic fauna in the Dutch sector of the North Sea in 2003 and a comparison with previous data, NIOZ-RAPPORT, 2001-2, 97, 2001.
 - Daewel, U. and Schrum, C.: Low-frequency variability in North Sea and Baltic Sea identified through simulations with the 3-D coupled physical-biogeochemical model ECOSMO, Earth System Dynamics, 8, 801–815, https://doi.org/10.5194/esd-8-801-2017, 2017.
- Daewel, U., Schrum, C., and MacDonald, J. I.: Towards end-to-end (E2E) modelling in a consistent NPZD-F modelling framework (ECOSMO E2E-v1.0): Application to the North Sea and Baltic Sea, Geoscientific Model Development, 12, 1765–1789, https://doi.org/10.5194/gmd-12-1765-2019, 2019.
 - Dijkstra, J. A., Buckman, K. L., Ward, D., Evans, D. W., Dionne, M., and Chen, C. Y.: Experimental and Natural Warming Elevates Mercury Concentrations in Estuarine Fish, PLOS ONE, 8, e58 401, https://doi.org/10.1371/JOURNAL.PONE.0058401, 2013.

- 610 Dufour, S. C.: Bivalve Chemosymbioses on Mudflats, Mudflat Ecology, pp. 169–184, https://doi.org/10.1007/978-3-319-99194-8_7, 2018.
 - Durnford, D., Dastoor, A., Figueras-Nieto, D., and Ryjkov, A.: Long range transport of mercury to the Arctic and across Canada, Atmos. Chem. Phys, 10, 6063–6086, https://doi.org/10.5194/acp-10-6063-2010, 2010.
 - Dutton, J. and Fisher, N. S.: Bioavailability of sediment-bound and algal metalsto killifish Fundulus heteroclitus, Aquatic biology, 16, 85–96, 2012.
- Egbert, G. D. and Erofeeva, S. Y.: Efficient Inverse Modeling of Barotropic Ocean Tides, Journal of Atmospheric and Oceanic Technology, 19, 183–204, https://doi.org/10.1175/1520-0426(2002)019<0183:EIMOBO>2.0.CO;2, 2002.
 - Eklöf, J., Austin, , Bergström, U., Donadi, S., Eriksson, B. D., Hansen, J., and Sundblad, G.: Size matters: Relationships between body size and body mass of common coastal, aquatic invertebrates in the Baltic Sea, PeerJ, 2017, e2906, https://doi.org/10.7717/PEERJ.2906/SUPP-1, 2017.
- Evers, D. C., Egan Keane, S., Basu, N., and Buck, D.: Evaluating the effectiveness of the Minamata Convention on Mercury: Principles and recommendations for next steps, https://doi.org/10.1016/j.scitotenv.2016.05.001, 2016.
 - Garcia H.E., Boyer T.P., Baranova O.K., Locarnini R.A., Mishonov A.V., Grodsky A., Paver C.R., Weathers K.W., Smolyar I.V., Reagan J.R., Seidov D., and Zweng M.W.: World Ocean Atlas 2018: Product Documentation. A. Mishonov, Technical Editor., 2019.
 - GEBCO Bathymetric Compilation Group: The GEBCO_2020 Grid a continuous terrain model of the global oceans and land., Tech. rep., https://doi.org//10.5285/a29c5465-b138-234d-e053-6c86abc040b9, 2020.

625

- Genchi, G., Sinicropi, M. S., Carocci, A., Lauria, G., and Catalano, A.: Mercury Exposure and Heart Diseases, International Journal of Environmental Research and Public Health, 14, 74, https://doi.org/10.3390/IJERPH14010074, 2017.
- Geyman, B. M., Streets, D. G., Olson, C. I., Thackray, C. P., Olson, C. L., Schaefer, K., Krabbenhoft, D. P., and Sunderland, E. M.: Cumulative Anthropogenic Impacts of Past and Future Emissions and Releases on the Global Mercury Cycle, Environmental Science and Technology, 59, 8578–8590, https://doi.org/10.1021/ACS.EST.4C13434/SUPPL_FILE/ES4C13434_SI_001.PDF, 2025.
- Ghodrati Shojaei, M., Gutow, L., Dannheim, J., Rachor, E., Schröder, A., and Brey, T.: Common trends in German Bight benthic macrofaunal communities: Assessing temporal variability and the relative importance of environmental variables, Journal of Sea Research, 107, 25–33, https://doi.org/10.1016/j.seares.2015.11.002, 2016.
- Gorokhova, E. and Hansson, S.: Elemental composition of Mysis mixta (Crustacea, Mysidacea) and energy costs of reproduction and embryogenesis under laboratory conditions, Journal of Experimental Marine Biology and Ecology, 246, 103–123, https://doi.org/10.1016/S0022-0981(99)00173-2, 2000.
 - Haitzer, M., Aiken, G. R., and Ryan, J. N.: Binding of mercury(II) to dissolved organic matter: the role of the mercury-to-DOM concentration ratio, Environmental science & technology, 36, 3564–3570, https://doi.org/10.1021/ES025699I, 2002.
- Harada, M.: Minamata Disease: Methylmercury Poisoning in Japan Caused by Environmental Pollution, Critical Reviews in Toxicology, 25, 1–24, https://doi.org/10.3109/10408449509089885, 1995.
 - Heip, C., Basford, D., Craeymeersch, J. A., Dewarumez, J.-m., Dorjes, J., de Wilde, P., Duineveld, G., Eleftheriou, A., J Herman, P. M., Niermann, U., Kingston, P., Kiinitzer, A., Rachor, E., Rumohr, H., Soetaert, K., Soltwedel Heip, T., Wilde, d., Heip A Craeymeersch, C. J., Soetaert, a., Laboratory, M., and Kiinitzer, S. A.: Trends in biomass, density and diversity of North Sea macrofauna, ICESJ. mar. Sci, 49, 13–22, https://doi.org/10.1093/icesjms/49.1.13, 1992.
- Jensen, S. and Jernelov, A.: Biological Methylation of Mercury in Aquatic Organisms, Nature, 223, 753–754, 1969.
 - Jurkiewicz-Karnkowska, E.: Some Aspects of Nitrogen, Carbon and Calcium Accumulation in Molluscs from the Zegrzyński Reservoir Ecosystem, Polish Journal of Environmental Studies, 14, 173–177, 2005.

- Krause-Jensen, D., Markager, S., and Dalsgaard, T.: Benthic and Pelagic Primary Production in Different Nutrient Regimes, Estuaries and Coasts, 35, 527–545, https://doi.org/10.1007/s12237-011-9443-1, 2012.
- 650 Lee, C. S. and Fisher, N. S.: Methylmercury uptake by diverse marine phytoplankton, Limnology and Oceanography, 61, 1626–1639, https://doi.org/10.1002/lno.10318, 2016.
 - Lin, H., Ascher, D. B., Myung, Y., Lamborg, C. H., Steven, Hallam, J., Gionfriddo, C. M., Kathryn, Holt, E., and Moreau, J. W.: Mercury methylation by metabolically versatile and cosmopolitan marine bacteria, The ISME Journal, 15, 1810–1825, https://doi.org/10.1038/s41396-020-00889-4, 2021.
- Lønborg, C., Carreira, C., Abril, G., Agustí, S., Amaral, V., Andersson, A., Arístegui, J., Bhadury, P., Bif, M. B., Borges, A. V., Bouillon, S., Calleja, M. L., Cotovicz, L. C., Cozzi, S., Doval, M., Duarte, C. M., Eyre, B., Fichot, C. G., García-Martín, E. E., Garzon-Garcia, A., Giani, M., Gonçalves-Araujo, R., Gruber, R., Hansell, D. A., Hashihama, F., He, D., Holding, J. M., Hunter, W. R., Ibánhez, J. S. P., Ibello, V., Jiang, S., Kim, G., Klun, K., Kowalczuk, P., Kubo, A., Lee, C. W., Lopes, C. B., Maggioni, F., Magni, P., Marrase, C., Martin, P., McCallister, S. L., McCallum, R., Medeiros, P. M., Morán, X. A. G., Muller-Karger, F. E., Myers-Pigg, A., Norli, M., Oakes, J. M.,
- Osterholz, H., Park, H., Lund Paulsen, M., Rosentreter, J. A., Ross, J. D., Rueda-Roa, D., Santinelli, C., Shen, Y., Teira, E., Tinta, T., Uher, G., Wakita, M., Ward, N., Watanabe, K., Xin, Y., Yamashita, Y., Yang, L., Yeo, J., Yuan, H., Zheng, Q., and Álvarez-Salgado, X. A.: A global database of dissolved organic matter (DOM) concentration measurements in coastal waters (CoastDOM v1), Earth System Science Data, 16, 1107–1119, https://doi.org/10.5194/ESSD-16-1107-2024, 2024.
- Madgett, A. S., Yates, K., Webster, L., McKenzie, C., and Moffat, C. F.: The concentration and biomagnification of trace metals and metalloids across four trophic levels in a marine food web, Marine Pollution Bulletin, 173, 112 929, https://doi.org/10.1016/j.marpolbul.2021.112929, 2021.
 - Mason, R. P., Reinfelder, J. R., and Morel, F. M.: Uptake, toxicity, and trophic transfer of mercury in a coastal diatom, Environmental Science and Technology, 30, 1835–1845, https://doi.org/10.1021/es950373d, 1996.
- McClelland, C., Chételat, J., Conlan, K., Aitken, A., Forbes, M. R., and Majewski, A.: Methylmercury dietary pathways and bioaccumulation in Arctic benthic invertebrates of the Beaufort Sea, Arctic Science, 10, 305–320, https://doi.org/10.1139/AS-2023-0021/ASSET/IMAGES/AS-2023-0021 TAB4.GIF, 2024.
 - Metian, M., Pouil, S., Dupuy, C., Teyssié, J.-L., Warnau, M., and Bustamante, P.: Influence of food (ciliate and phytoplankton) on the trophic transfer of inorganic and methyl-mercury in the Pacific cupped oyster Crassostrea gigas, Environmental Pollution, 257, https://doi.org/10.1016/j.envpol.2019.113503ï, 2020.
- 675 Muhaya, B. B. M., Leermakers, M., and Baeyens, W.: Total mercury and methylmercury in sediments and in the polychaete nereis diversicolor at groot buitenschoor (scheldt estuary, belgium), Water, Air, and Soil Pollution, 94, 109–123, 1997.
 - Nfon, E., Cousins, I. T., Järvinen, O., Mukherjee, A. B., Verta, M., and Broman, D.: Trophodynamics of mercury and other trace elements in a pelagic food chain from the Baltic Sea, https://doi.org/10.1016/j.scitotenv.2009.08.032, 2009.
- Olinger, L. K., Strangman, W. K., McMurray, S. E., and Pawlik, J. R.: Sponges With Microbial Symbionts Transform Dissolved Organic Matter and Take Up Organohalides, Frontiers in Marine Science, 8, 665 789, https://doi.org/10.3389/FMARS.2021.665789/BIBTEX, 2021.
 - Orani, A. M., Vassileva, E., Azemard, S., and Thomas, O. P.: Comparative study on Hg bioaccumulation and biotransformation in Mediterranean and Atlantic sponge species, Chemosphere, 260, 127515, https://doi.org/10.1016/J.CHEMOSPHERE.2020.127515, 2020.
- Outridge, P. M., Mason, R. P., Wang, F., Guerrero, S., and Heimbürger-Boavida, L. E.: Updated Global and Oceanic Mercury Budgets for the United Nations Global Mercury Assessment 2018, https://doi.org/10.1021/acs.est.8b01246, 2018.

- Pacyna, E. G., Pacyna, J. M., Steenhuisen, F., and Wilson, S.: Global anthropogenic mercury emission inventory for 2000, Atmospheric Environment, 40, 4048–4063, https://doi.org/10.1016/j.atmosenv.2006.03.041, 2006.
- Pan, K. and Wang, W. X.: Mercury accumulation in marine bivalves: Influences of biodynamics and feeding niche, Environmental Pollution, 159, 2500–2506, https://doi.org/10.1016/J.ENVPOL.2011.06.029, 2011.
- 690 Pickhardt, P. C., Stepanova, M., and Fisher, N. S.: Contrasting uptake routes and tissue distributions of inorganic and methylmercury in mosquitofish (Gambusia affinis) and redear sunfish (Lepomis microlophus), Environmental Toxicology and Chemistry, 25, 2132–2142, https://doi.org/10.1897/05-595R.1, 2006.
 - Richardson, K., Bo, F., Richardson, P., Pedersen, B., and Richardson, K.: Estimation of new production in the North Sea: consequences for temporal and spatial variability of phytoplankton, Tech. rep., 1998.
- 695 Schartup, A. T., Qureshi, A., Dassuncao, C., Thackray, C. P., Harding, G., and Sunderland, E. M.: A Model for Methylmercury Uptake and Trophic Transfer by Marine Plankton, Environ. Sci. Technol, 52, 18, https://doi.org/10.1021/acs.est.7b03821, 2018.
 - Sheehan, M. C., Burke, T. A., Navas-Acien, A., Breysse, P. N., Mcgready, J., and Fox, M. A.: Systematic reviews Global methylmercury exposure from seafood consumption and risk of developmental neurotoxicity: a systematic review, Bull World Health Organ, 92, 254–269, https://doi.org/10.2471/BLT.12.116152, 2014.
- 700 Silberberger, M. J., Renaud, P. E., Kröncke, I., and Reiss, H.: Food-web structure in four locations along the European shelf indicates spatial differences in ecosystem functioning, Frontiers in Marine Science, 5, 300 569, https://doi.org/10.3389/FMARS.2018.00119/BIBTEX, 2018.
 - Sommar, J., Osterwalder, S., and Zhu, W.: Recent advances in understanding and measurement of Hg in the environment: Surface-atmosphere exchange of gaseous elemental mercury (Hg0), Science of The Total Environment, 721, 137648, https://doi.org/10.1016/J.SCITOTENV.2020.137648, 2020.

- Tesán Onrubia, J. A., Petrova, M. V., Puigcorbé, V., Black, E. E., Valk, O., Dufour, A., Hamelin, B., Buesseler, K. O., Masqué, P., Le Moigne, F. A., Sonke, J. E., Rutgers Van Der Loeff, M., and Heimbürger-Boavida, L. E.: Mercury Export Flux in the Arctic Ocean Estimated from 234Th/238U Disequilibria, ACS Earth and Space Chemistry, 4, 795–801, https://doi.org/10.1021/acsearthspacechem.0c00055, 2020.
- Trasande, L., Schechter, C., Haynes, K. A., Landrigan, P. J., and Acad Sci, A. N.: Applying Cost Analyses to Drive Policy That Protects

 Children Mercury as a Case Study, https://doi.org/10.1196/annals.1371.034, 2006.
 - Tsui, M. T. and Wang, W. X.: Uptake and Elimination Routes of Inorganic Mercury and Methylmercury in Daphnia magna, Environmental Science and Technology, 38, 808–816, https://doi.org/10.1021/es034638x, 2004.
 - UNEP: Global Mercury Assessment 2013: Sources, Emissions, Releases and Environmental Transport., UNEP Chemicals Branch, Geneva, Switzerland, 2013.
- Wang, W. and Wong, R.: Bioaccumulation kinetics and exposure pathways of inorganic mercury and methylmercury in a marine fish, the sweetlips Plectorhinchus gibbosus, Marine Ecology Progress Series, 261, https://doi.org/10.3354/meps261257, 2003.
 - Weil, J., Trudel, M., Tucker, S., Brodeur, R. D., and Juanes, F.: Percent ash-free dry weight as a robust method to estimate energy density across taxa, Ecology and Evolution, 9, 13 244–13 254, https://doi.org/10.1002/ECE3.5775, 2019.
- Wouters, H., Berckmans, J., Maes, R., Vanuytrecht, E., and De Ridder, K.: Global bioclimatic indicators from 1979 to 2018 derived from reanalysis, version 1.0, Copernicus Climate Change Service (C3S) Climate Data Store (CDS), DOI: 10.24381/cds.bce175f0, 2021.
 - Zaferani, S. and Biester, H.: Mercury Accumulation in Marine Sediments A Comparison of an Upwelling Area and Two Large River Mouths, Frontiers in Marine Science, 8, 732 720, https://doi.org/10.3389/FMARS.2021.732720/BIBTEX, 2021.

- Zhang, Y., Song, Z., Huang, S., Zhang, P., Peng, Y., Wu, P., Gu, J., Dutkiewicz, S., Zhang, H., Wu, S., Wang, F., Chen, L., Wang, S., and Li, P.: Global health effects of future atmospheric mercury emissions, Nature Communications 2021 12:1, 12, 1–10, https://doi.org/10.1038/s41467-021-23391-7, 2021.
 - Zhao, C., Daewel, U., and Schrum, C.: Tidal impacts on primary production in the North Sea, Earth System Dynamics, 10, 287–317, https://doi.org/10.5194/esd-10-287-2019, 2019.